Earth History and PALAEOGEOGRAPHY

Trond H. Torsvik and L. Robin M. Cocks

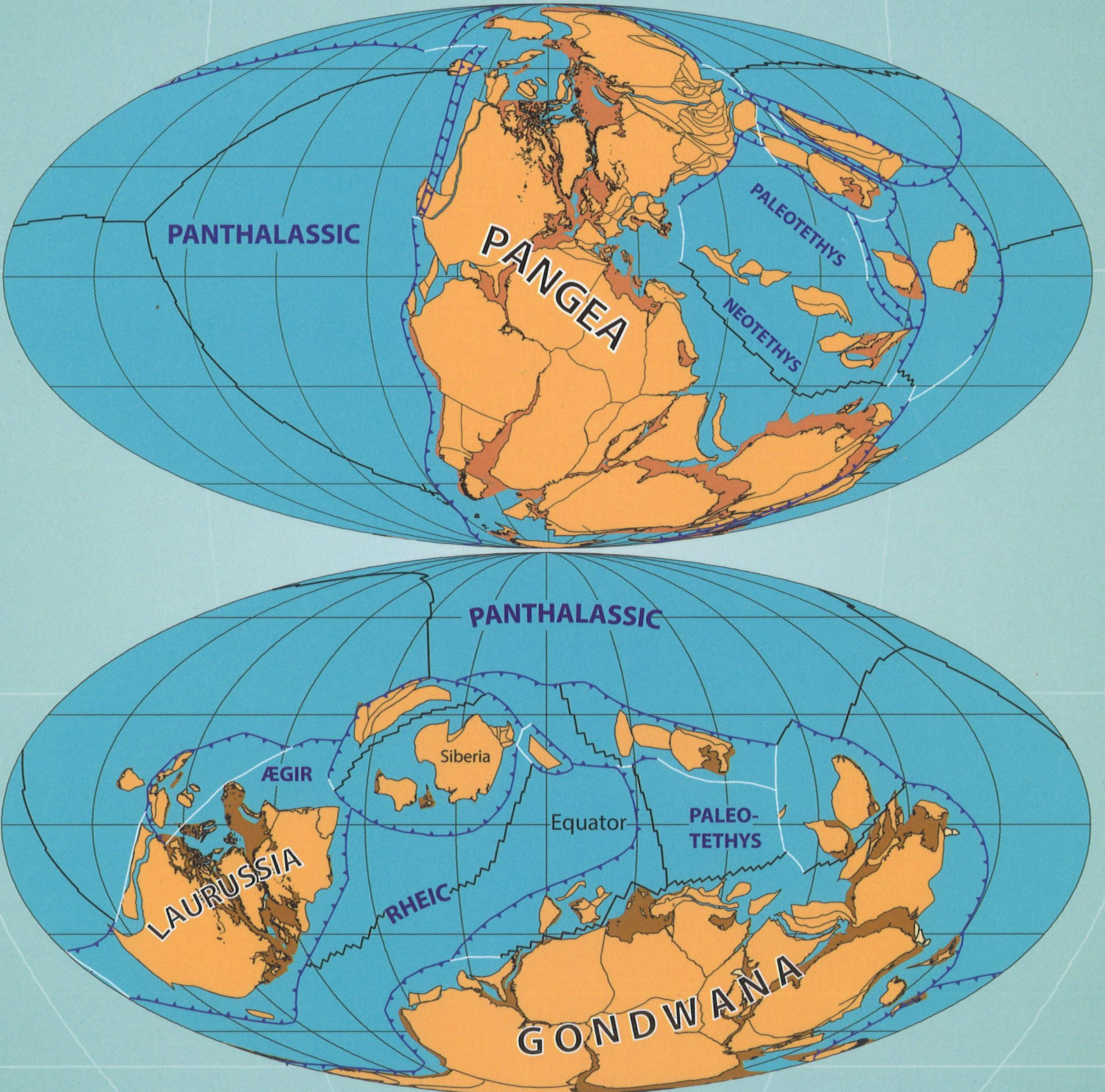

1 Introduction

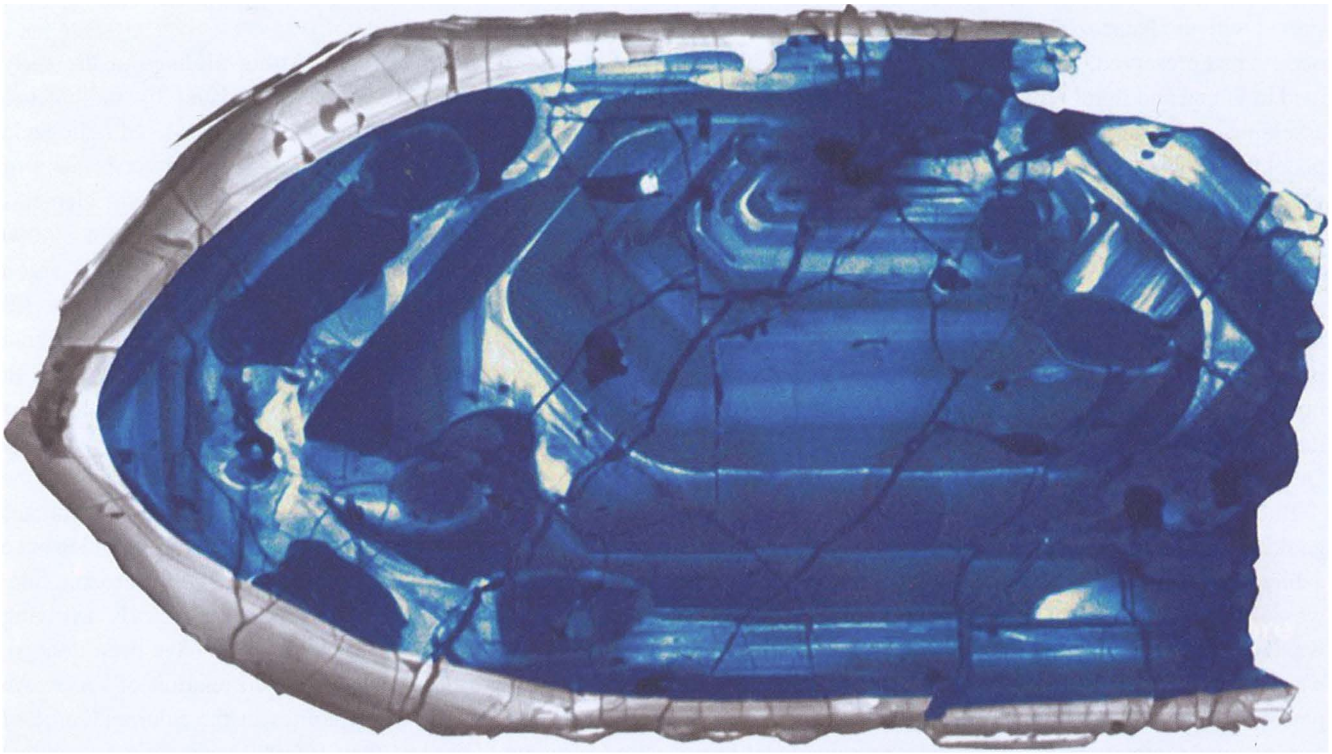

The oldest known zircon on Earth is 4.374 ± 0.006 billion years old. This grain is from the Jack Hills in Western Australia and is about 200 million years younger than the age of the Earth, and is probably a remnant of the oldest continental crust. Credit: John Valley, University of Wisconsin/Nature Geoscience.

When the Earth is viewed from space on a cloudless day, all that can be seen are the edges of lands, seas, and ice caps, all of which can be objectively mapped. From further geophysical exploration, the identities and margins of the oceans and the continental lithosphere which lie beside and below them today can also be discovered. However, how and when all those margins have changed through geological time becomes progressively less easy to discover and also less objective, since an uncertain number of the plates and their included oceanic and continental lithosphere have disappeared by subduction into the Earth's interior. In addition, much of the lithosphere has been distorted through tectonic processes, in many places very heavily.

Our chief aim in writing this book is to interpret, decipher, and describe the complex history of our planet over the most recent half-billion years and the processes through which it has changed, and to compile maps of the distribution of the many tectonic plates through that time, and also show where the lands and seas were situated over that long period. As is usual with narration, we start at the beginning and carry on progressively through time as it elapsed, but the result of that natural sequence is to commence by discussing the periods over which we have the fewest quantitative constraints on Earth's old geography, and thus our geographical reconstructions gradually become more accurate as time continues up to the present day.

The periods into which geological time is divided are shown on the endpapers within this book's covers. The history of the Earth falls naturally into two very unequal divisions: the Precambrian, in which there are no fossils of use in determining the positions of the former continents, and which, including the origin of the planet, is only summarised here in Chapter 4. The Precambrian was followed by the Phanerozoic at 541 million years ago (Ma), and the latter started with the Palaeozoic, from which there is no old *in situ* ocean crust preserved, but this is when the biota was distributed in faunal and floral provinces which are very relevant in assessing oceanic separations in the absence of much useful geophysical data (apart from palaeomagnetism). The boundary between the Palaeozoic and the overlying Mesozoic to the present day was at 252 Ma, after which the ocean-floor magnetic stripes and other useful geophysical data become progressively more abundant and objective, but when the biota, although interesting in its evolutionary development, is again of no primary help in deciphering the palaeogeography. Thus there are separate chapters here for each of the main geological systemic periods from the Cambrian to the Quaternary (Chapters 5 to 15).

But what are the stepping stones, which cover many geological and geophysical disciplines, by which we can achieve our aims? After this brief introduction, in Chapter 2 we describe the varied and often independent methods that we have used to reconstruct old lands and seas. In Chapter 3 we list the 268 unit areas among the many making up our planet which are the ones we have used in the construction of our kinematic computer-generated palaeogeographical maps through time, with a very brief sketch of their geological constitutions. Each of those units, which vary in size from large continents to small terranes, can be downloaded digitally from www.earthdynamics.org/earthhistory, together with a digital rotation file and various other files, which can be used by anyone to make their own reconstructions with GPlates (www.gplates.org) for any area and at any given time for the past 540 million years, with no fees involved but acknowledgements requested.

Over the past billion years, our planet's climate has fluctuated wildly between hot and cold temperatures, some so extreme that any life has been scarcely possible. Thus, as well as mentioning those climates during the individual periods in Chapters 4 to 15, the final Chapter 16 brings together the many factors which affect and support the Earth's climate, and also describes how and why that climate has changed so much during the half-billion years and how it has come to be what it is today. Unfortunately, that deeper time perspective appears to be lacking in many modern-day climate scientists and politicians.

But underlying all that, our book and all of geological thinking depends on knowing how long ago each past event occurred. So that we can comprehend and evaluate the number of years over which the many changes of the Earth's surface and interior have taken place since its origin, and from that the rates of those changes, it is essential to know objectively the amount of time available for their progression. Thus a reliable primary geochronology is critical for underpinning our work.

Since the pioneer work by Arthur Holmes in the early twentieth century, rocks have been dated by radiometric methods, using a great variety of the longer-lived radiogenic isotopes, some of whose half-lives extend over billions of years (Torsvik & Cocks, 2012). The most useful elements have been found to be carbon for the most recent 30,000 years, and a variety of others, including argon–argon ($^{40}Ar/^{39}Ar$) and uranium–lead (U/Pb), for older rocks. All radiometric ages have errors calculated individually, which are given in the original papers, and most are published with dates including proportions within a million years, but, so that this text can flow relatively unimpeded, we have rounded all ages earlier than the Cenozoic (66 Ma) to the nearest one million years, and do not quote the published error ranges here. But, although lacking the objective numbers which have come from geochronology, in much of the Phanerozoic finer time divisions exist through the use of quickly evolving animals and plants from which biozones have been defined, and which have been used in the correlation of rocks. An example of the latter is graptolites in the Silurian, some of whose biozones are less than 100,000 years long, in contrast to the radiometric ages for that period, which are not accurate to within about one-third of a million years.

The overall time scale on which our work depends is inside the endpapers of this book, where the dates for the bases of the major time units are shown, most of which have now been standardised by the International Union of Geological Sciences (IUGS) Commission on Stratigraphy (Cohen et al., 2013).

It has been difficult to know how many references should best be cited. Many textbooks are frustrating in their relative lack, or sometimes even complete absence, of references, whilst research papers usually include at least one reference to support every fresh statement, and often far too many more, particularly to papers written by friends of the authors. This has led us to compromise, and we apologise both to current workers for the omission of precise citation of much invaluable work, and also to those earlier scientists on whose shoulders we all stand, particularly since we have tended to refer to summary articles in many places here, rather than to the many papers which underpin those works.

2 Methods for Locating Old Continents and Terranes

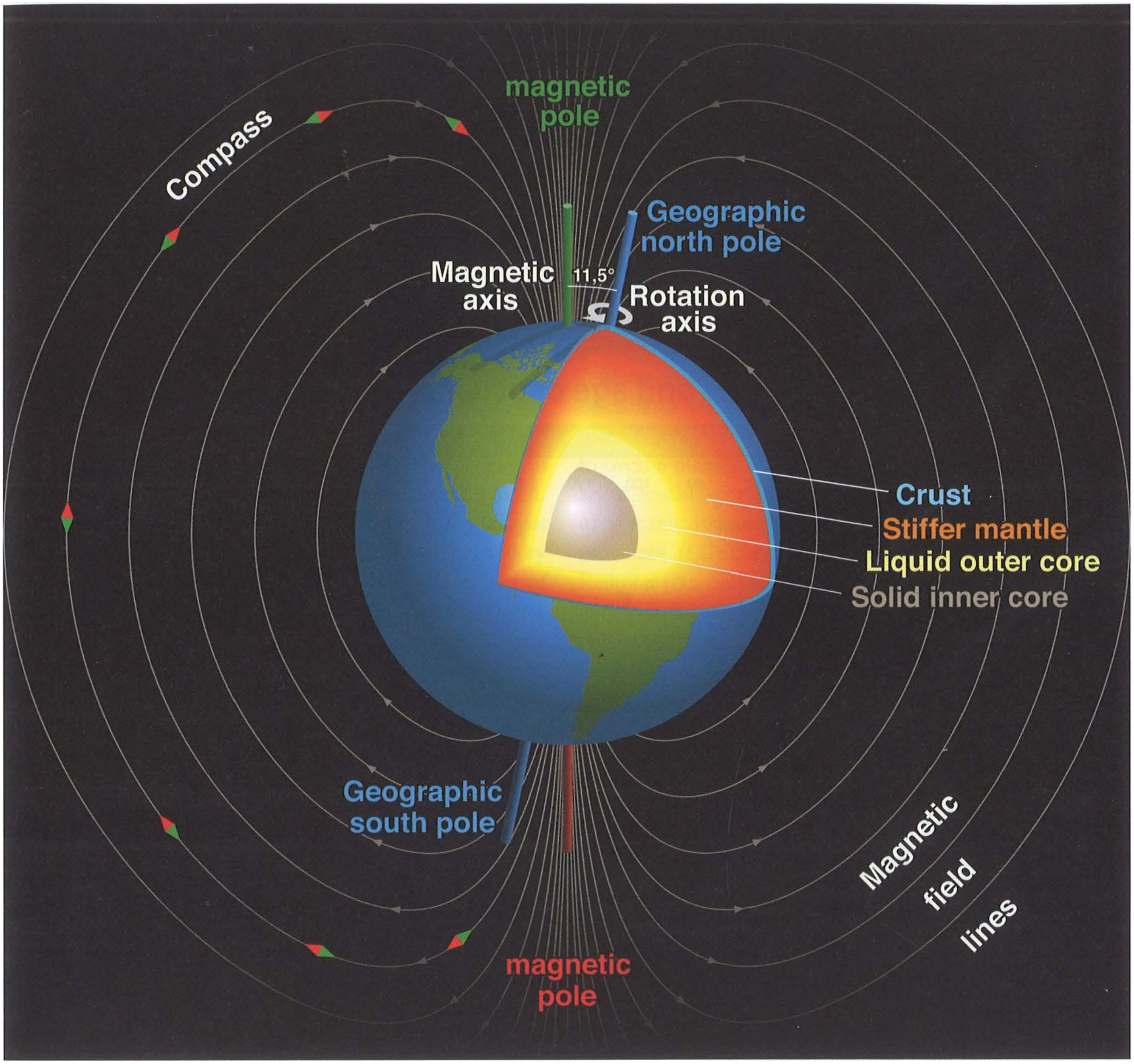

From the vantage point of geological time, the Earth is best seen as a giant heat engine. The decay of radioactive nuclides in the deep interior provides energy for its most fundamental dynamical processes: convection in both the liquid outer core and the stiffer (solid) but slowly deforming mantle. Under the influence of the Earth's rotation, the electrically conductive outer core generates the Earth's magnetic field. This field shelters us from cosmogenic radiation, modulates atmospheric escape, and provides guidance for many migratory species. The Earth's ancient magnetic field provided one of the fundamental markers used to document the motion of the continents and evolution of the Earth. Changes in ancient magnetic polarity at irregular intervals are recorded in the surface rock record, and over some fifty years such palaeomagnetic data have been used to create the geomagnetic time scale, to firmly document sea-floor spreading, to validate plate tectonics, and to reconstruct vanished supercontinents. The magnetic poles differ from the geographical poles because the magnetic axis is inclined relative to the geographical (rotation) axis (today ~11.5°). The magnetic axis, however, is rotating slowly around the geographical axis and, over a period of a few thousand years, the averaged magnetic poles have corresponded reasonably well with the geographical poles. Credit: Furian/Shutterstock.

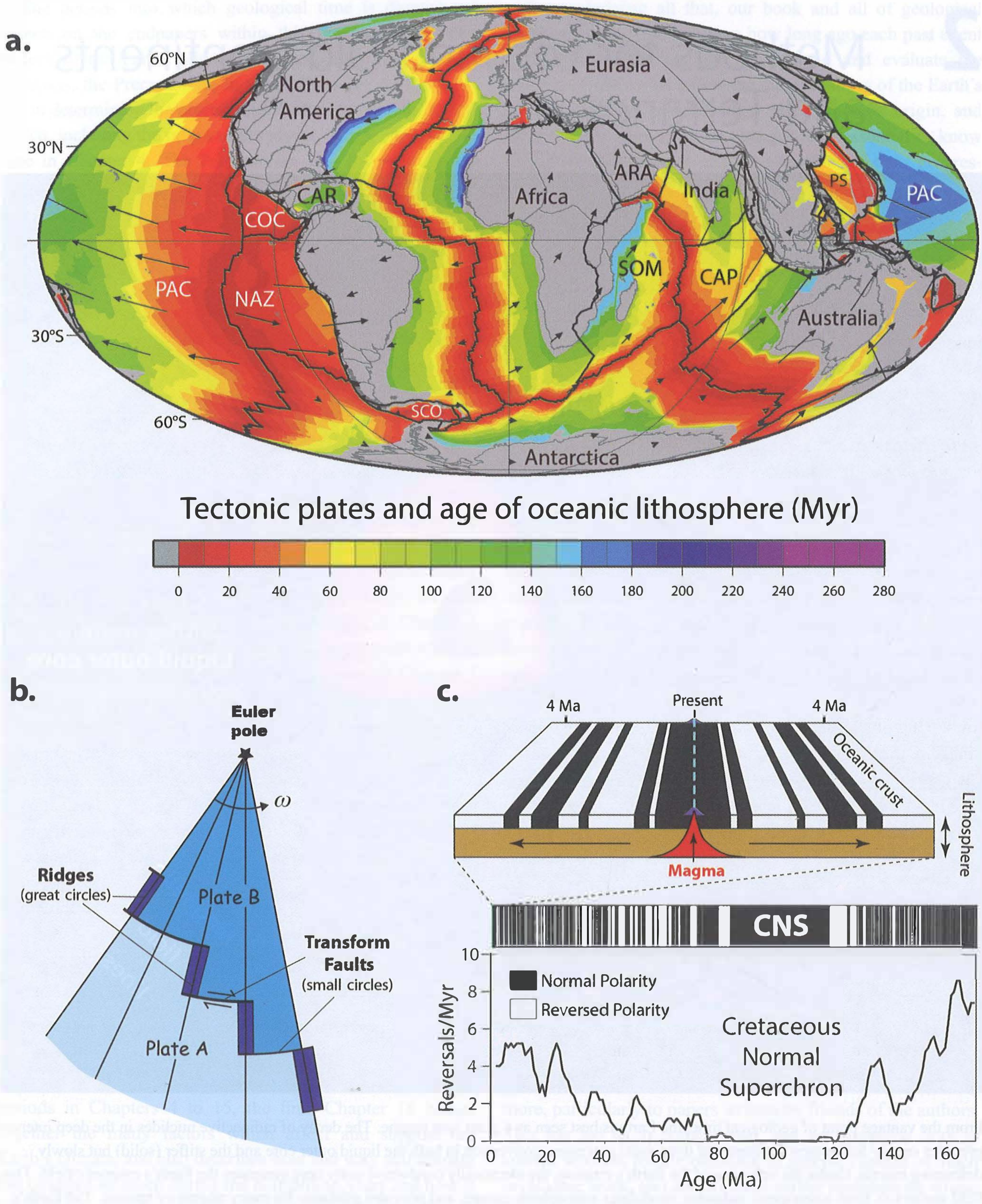

Fig. 2.1 (a) Present-day distribution of tectonic plates. Base map shows the modelled age of oceanic crust; warm (red) colours indicate young sea floor (close to the spreading axis), while cold (blue/violet) colours indicate old oceanic crust. The oldest preserved oceanic crust (possibly 195 million years old: Early Jurassic) is found, among other places, in the Central Atlantic between North America

Over the last century, our portrayal of the movement and deformation of the Earth's outer layer evolved from the hypothesis of Continental Drift (1912) into Sea-Floor Spreading (1962) and then to the paradigm of Plate Tectonics (1967). The word 'tectonics' comes from Greek and means 'to build', and plate tectonics is as fundamentally unifying to the Earth Sciences as Darwin's (1859) Theory of Evolution is to the Life Sciences. Most of this book describes how the geography of the Earth has changed over geological time. However, this chapter sets out the various methods by which the positions of old continents can be deduced, most of them completely independent from each other. It is important to bear in mind that the geographical areas (Chapter 3) in older times shown on our reconstructions (Chapters 4–15) rarely reflect the real shape of those continents at those individual times in the past, since their margins have been much changed by subsequent tectonic events.

Plate reconstructions at successive intervals in geological time are the result of a reiterative process using a wealth of methods. The relative positions of continents are commonly determined from ocean-floor magnetic anomalies (since the Jurassic) and fracture-zone geometries, analysis of continent–ocean boundaries, palaeomagnetic poles, and other geological and geophysical data. Continents and terranes are then reconstructed to their ancient positions on the globe using hotspot trails (since the Cretaceous) or palaeomagnetic data, and by identifying and discriminating between the distributions of various fauna and flora in their various provinces at different times. These biological distributions can indicate if terranes with similar biota were close to one another or were separate. The distribution of key sediments, such as glacial deposits, coal, and evaporites, can also be useful, but they are largely latitudinally determined rather than terrane-specific.

Plates and Plumes

Plate tectonics describes how the Earth's lithosphere (the crust and upper mantle) is constructed from a dozen large and many smaller rigid blocks that move in relation to each other (Fig. 2.1a). It is a captivating story of oceanic and thicker continental plates that move across the Earth's surface, and how they glide apart forming new oceanic crust (divergent plate boundaries), collide to form mountain belts (convergent boundaries), or move sideways in relation to each other (transform boundaries). The motions of rigid plates can be described by Euler rotations (Fig. 2.1b). Plate velocities range from about 1 to 15 cm/yr, and earthquakes and volcanic eruptions close to the plate boundaries are key elements of the plate tectonic paradigm. Under the influence of the Earth's rotation, the electrically conductive outer core generates the Earth's magnetic field. The history of that ancient magnetic field provides one of the fundamental clues used to document the motion of the continents and evolution of the Earth. Changes in ancient magnetic polarity at irregular intervals are recorded in the surface rock record, and those palaeomagnetic data have been used to create the geomagnetic time scale (Fig. 2.1c).

Hotspots can be referred to as volcanism unrelated to plate boundaries and rifts, and many intra-plate hotspots such as the one beneath Hawaii (Wilson, 1963) have been suggested to overlie plumes that originated at the core mantle boundary. A few hotspots also lie at the ends of plume trails (chains of volcanic islands) which are connected to large igneous provinces (LIPs), e.g. the Tristan (Paraná Etendeka) and Reunion (Deccan) hotspots. The Hawaii Hotspot was probably also linked to a starting LIP, which was long subducted (Chapters 13 and 14), whilst the New England Hotspot lies at the end of a plume trail that was connected with Jurassic kimberlite volcanism in continental north-eastern America. Many hotspots are clearly intra-plate (e.g. in the Pacific and Africa, Fig. 2.2a) and therefore unrelated to plate tectonics, but some are located on or near a plate tectonic boundary.

The lowermost mantle is characterised by two large heterogeneities where shear-wave velocities are up to three per cent slower than in the surrounding mantle. Those thermochemical piles are near antipodal and equatorially centred

Fig. 2.1 (*cont.*) and North-West Africa, and linked to the very earliest breakup of the supercontinent of Pangea. Red lines denote subduction zones, black lines denote mid-ocean ridges and transform faults. Plate motions (moving hotspot frame) are shown as black arrows. ARA, Arabia; CAP, Capricorn; CAR, Caribbean; COC, Cocus; NAZ, Nazca; PAC, Pacific; PS, Philippine Sea; SCO, Scotia; SOM, Somalia (data from EARTHBYTE). (b) On a sphere the relationship between two plates (A and B in this example) is described by a rotation (Euler) pole (latitude, longitude, and angle) and the relative speed (ω) is commonly expressed in °/Myr. Spreading ridges define great circles, while ocean fracture zones (transform faults) define small circles. (c) Cartoon illustrating the formation of magnetic anomalies at a mid-ocean ridge and the marine magnetic anomaly polarity record and reversal frequency (10 Myr running mean based on data in Biggin et al., 2012). Reversal frequency peaked in the Jurassic (~150 170 Ma), but the most extreme geomagnetic behaviour was in the Cretaceous Normal Superchron (CNS) from 121 to 84 Ma (Late Jurassic to Mid–Late Cretaceous), when the field was of single polarity for almost 40 Myr. Two older Phanerozoic superchrons have also been suggested: the Permian–Carboniferous Kiaman Reverse Superchron (~265–310 Ma) and an Ordovician Reversed Superchron between about 460 and 490 Ma.

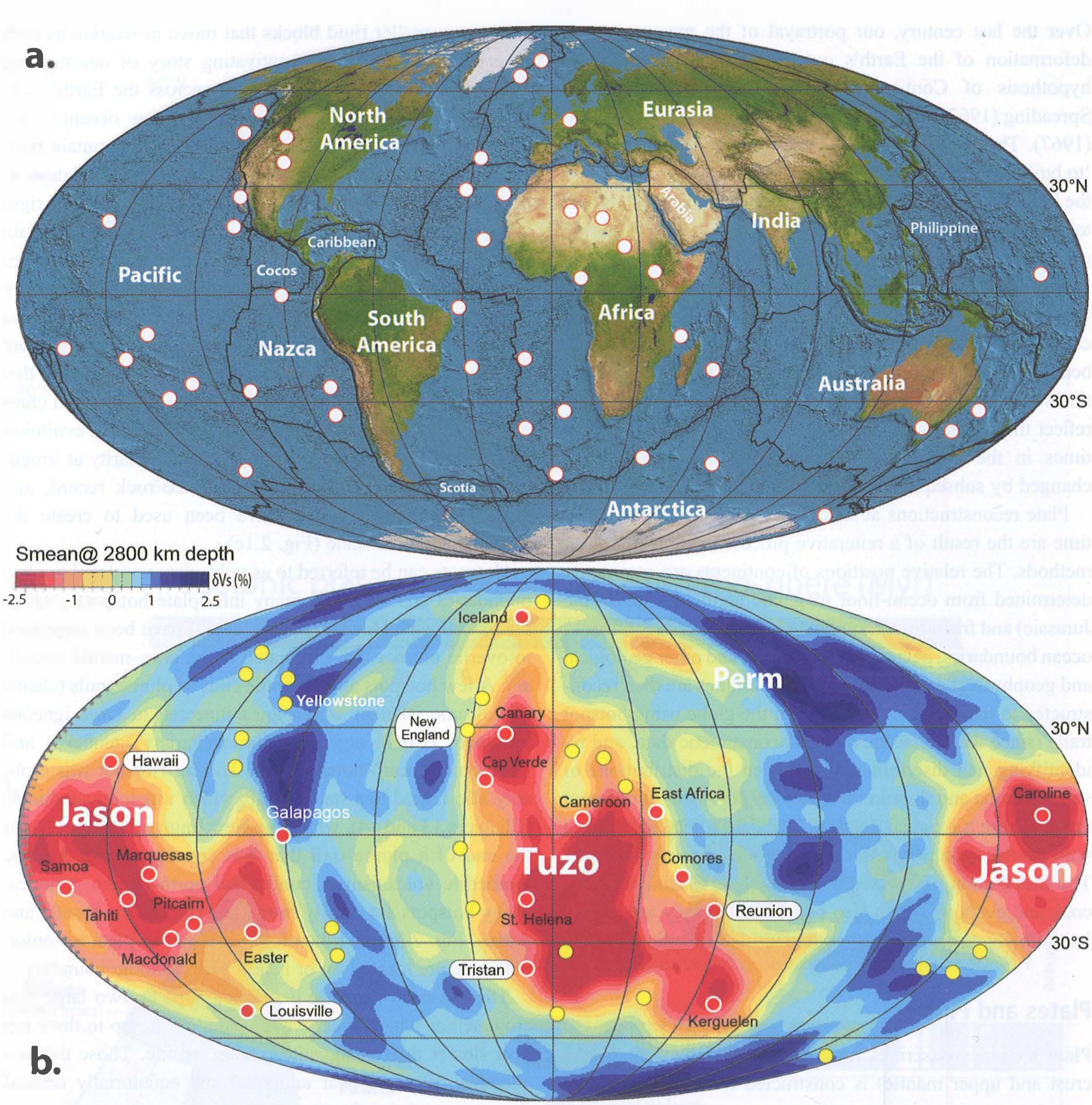

Fig. 2.2 (a) Main plate boundaries (black thick lines) and the distribution of hotspots (red circles with white filling; Steinberger, 2000) draped on a global map of topography and bathymetry. In plate tectonic theory, volcanism, deformation, and earthquakes should be confined mainly to regions near the plate boundaries. However, many hotspots are found within the plates (e.g. Pacific and African plates) which are not readily explained by plate tectonic processes. (b) Plot of hotspots as in (a) but draped on the SMEAN shear-wave velocity anomaly model at 2,800 km depth (Becker & Boschi, 2002). Velocity anomalies (δV_s) in percentage and red denote regions with low velocity. The lower mantle is characterised by two main zones of low shear-wave velocities, mainly beneath Africa (Tuzo) and the Pacific (Jason). In addition, a smaller one named Perm (which may alternatively be part of Tuzo) is located beneath Siberia. Many hotspots appear to overlie regions of slower than average shear-wave velocities (notably those associated with Tuzo) but there are clear exceptions (e.g. Yellowstone in North America). Those hotspots, thought to be sourced by deep plumes from the core–mantle boundary (primary and clearly resolved plumes in French & Romanowicz, 2015), are shown as white circles with red filling, whilst others of unknown origin are shown as yellow dots.

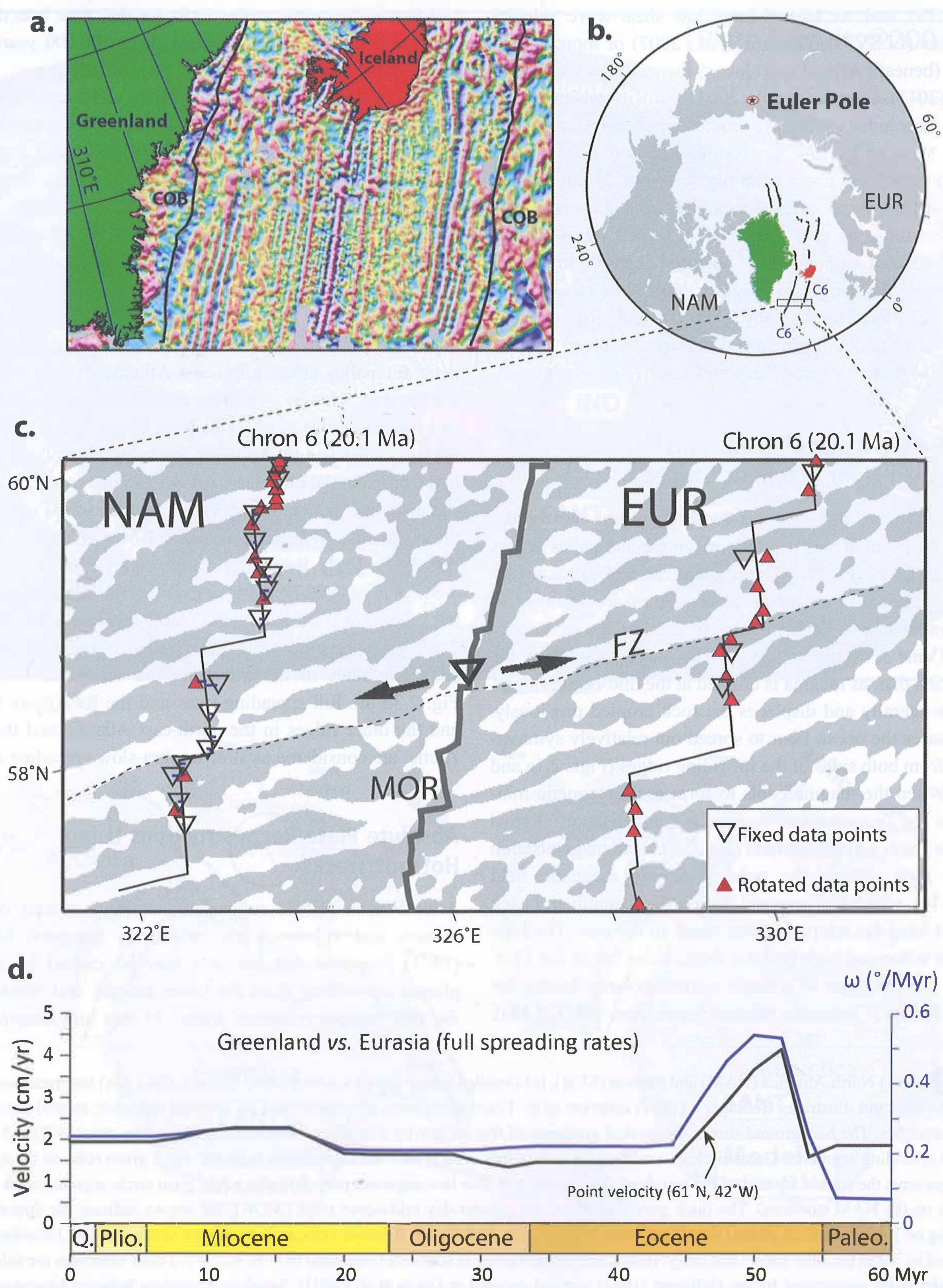

Fig. 2.3 (a) Magnetic anomaly grid of the north-east Atlantic south of Iceland. The thick black lines are Continent–Ocean Boundary transitions (COBs). (b) Example of marine magnetic anomaly interpretations (700 data points of Chron 6, C6) and resulting Euler pole (EP) (black star) and uncertainty ellipse (red contour around EP; enlarged three times so as to be visible on the map) for relative motion between

(Fig. 2.2b), and are termed large low shear-wave velocity provinces (LLSVPs) (Garnero et al., 2007) or more simply 'Tuzo' (beneath Africa) and 'Jason' (beneath the Pacific) by Burke (2011). Courtillot et al. (2003) and Ritsema and Allen (2003) concluded that only eight hotspots (Afar, Easter Island, Hawaii, Iceland, Louisville, Réunion, Samoa, and Tristan) potentially had a deep plume origin. Montelli et al. (2006) added three extra hotspots (Azores, Canary, and Tahiti) to those of deep origin, and Torsvik et al. (2006) pointed out that all hotspots of potential deep origin plot on or very near the margins of Tuzo or Jason. In a recent study using full-wave tomography, French and Romanowicz (2015) identified 20 primary or clearly resolved plumes (Fig. 2.2b) that all overlie Tuzo and Jason.

Relative Positions of Continents and Ocean Floor Magnetic Stripes

As long ago as the 1950s, scientists noticed the regular pattern of positive and negative magnetic anomalies across the ocean floors (Fig. 2.3a), and it was realised subsequently that the lines of those magnetic anomalies are arranged in sub-parallel stripes on both sides of each of the mid-ocean ridges (Vine & Matthews, 1963). That was explained by the realisation that, as magma is erupted at the mid-ocean ridges, it flows laterally and displaces the rock erupted previously. That causes the ocean floor to spread out relatively symmetrically from both sides of the spreading ridges (Figs. 2.1a and 2.3a). When the magma cools to form rock, magnetic minerals in the oceanic crust acquire a magnetisation aligned with the Earth's magnetic field (Fig. 2.9). That magnetisation in the rock reflects the polarity of the magnetic field (Fig. 2.1c), which has reversed from north to south and back again at irregular intervals many times in the past. The Late Jurassic witnessed high reversal frequencies but in the Cretaceous the field was of a single normal polarity lasting for almost 40 Myr (Cretaceous Normal Superchron, ~84–121 Ma), and thus no magnetic stripes exist for that time interval. On average, there has been a reversal every 200,000 years (five reversals per million years) during the past 10 Myr.

The matching of magnetic anomalies and fracture zones of the same age, corresponding to patterns of palaeo-ridge (great-circle) and palaeo-transform (small-circle) segments at any particular reconstruction time (Fig. 2.1b), is used to determine the relative motions between tectonic plates (Fig. 2.3b and c). The Hellinger (1981) method is most commonly used to derive best-fit rotations (Euler poles) from conjugate magnetic anomalies and fracture zone data (Fig. 2.3c), which are in turn used to derive spreading velocities between two plates. Figure 2.3 shows gridded magnetic anomalies in the north-east Atlantic from Iceland and southwards, with an example of fitting magnetic anomalies and fracture zones at around Chron 6 time (20.1 Ma) along the Reykjanes Ridge. Applying this method to all the identified Chrons in the north-east Atlantic (Gaina et al., 2002) one can calculate the relative speed back to the initial opening of the north-east Atlantic at around 54 Ma. Velocities peaked during the Early Eocene opening stage (about 0.5°/Myr or 4 cm/yr for a location along the southern Greenland margin), but otherwise have been quite stable at around 0.2°/Myr or 2 cm/yr. Spreading velocities are often reported as half-spreading rates in the literature; the values calculated in Fig. 2.3d are full spreading rates and the Reykjanes Ridge, and the other ridges in the north-east Atlantic and the high Arctic, are considered as slow to ultra-slow spreading ridges.

Absolute Plate Reconstructions Using Hotspot Tracks

After Wilson (1963) suggested that linear chains of seamounts and volcanoes are caused by hotspots, Morgan (1971) proposed that hotspots may be caused by mantle plumes up-welling from the lower mantle, and constructed the first hotspot reference frame. In that and later models

Fig. 2.3 (*cont.*) North America (NAM) and Eurasia (EUR). (c) Detailed image shows a subset of the Chron 6 (20.1 Ma) interpretation in the North Atlantic and illustrates Hellinger's (1981) criterion of fit. Fixed data points are represented by inverted triangles; rotated data points are red triangles. The background shows the vertical gradients of free air gravity that allow identification of fracture zones (FZ) and offsets between spreading segments. Great circles were fitted for data points in each individual spreading segment. For a given rotation the measure of fit represents the sum of squares of the weighted distances (short blue line segments perpendicular to the great circle segment shown as an example on the NAM isochron). The thick grey line shows the present-day mid-ocean ridge (MOR); the arrows indicate the direction of spreading on NAM and EUR plates (simplified from Torsvik et al., 2008b). (d) Relative velocity between the Greenland and Eurasian Plates expressed in °/Myr (ω, blue curve) and cm/yr (black curve) for a point in southern Greenland (61° N, 42° W). Those velocities are calculated from Euler poles determined by the Hellinger (1981) method detailed in Gaina et al. (2002). Sea-floor spreading between Greenland and Eurasia started at around 54 Ma, but before then there was a period of Late Cretaceous–Paleocene pre-drift extension, and therefore velocities are not zero before breakup. Velocities are calculated over a 5 Myr window and shown at 2 Myr intervals. Paleo., Paleocene; Plio., Pliocene; Q., Quaternary.

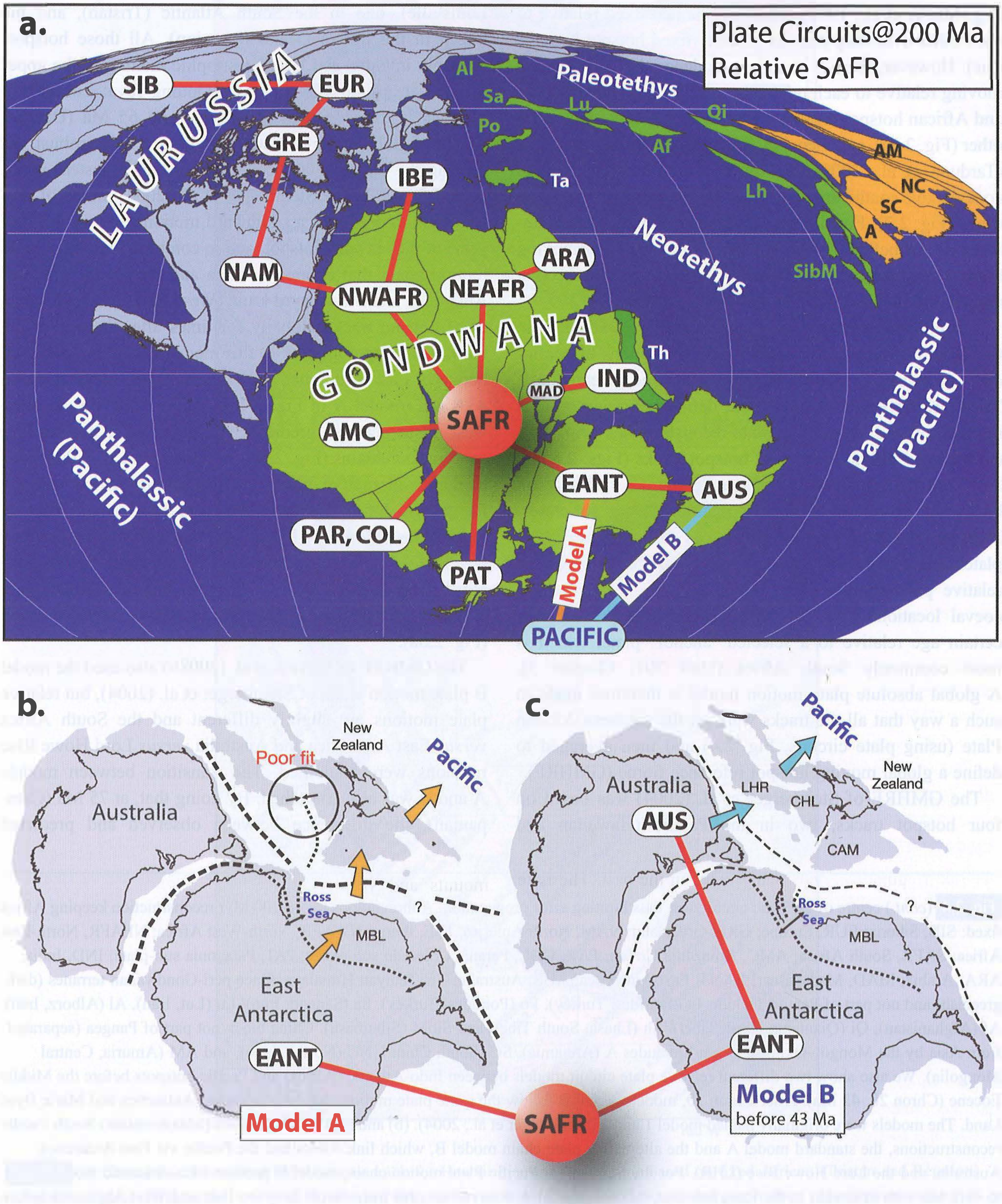

Fig. 2.4 (a) When building global plate motion models before the Cretaceous it is important to choose a plate as an initial reference that has undergone a small amount of longitudinal movement. Africa is the ideal candidate because it has remained extremely stable for the past 200 Myr, having mostly been surrounded by spreading centres since the Jurassic. Africa has the added advantage of being nearly in the

(e.g. Müller et al., 1993), plumes remained fixed relative to each other over long periods of time (fixed hotspot hypothesis). However, there is abundant evidence that hotspots are moving relative to each other; for example, the fixed Pacific and African hotspot reference frames do not agree with each other (Fig. 2.5a), and there is sound palaeomagnetic evidence (Tarduno et al., 2009) that the Hawaii Plume underwent considerable southward drift in Late Cretaceous to Paleogene times (Fig. 2.7). Fixed hotspot reference frames must therefore (at least before 40 Ma) be replaced by a mantle (moving hotspot) frame in which motions of hotspots in a convecting mantle are assumed (Steinberger et al., 2004).

Hotspot reference frame reconstructions are absolute in the sense that they constrain the ancient positions of continents (described by latitudes, longitudes, and orientations). There are three key elements that define a moving hotspot reference frame: (i) relative plate reconstructions (Fig. 2.4), (ii) the ages and geometries of hotspot tracks (Figs. 2.5 and 2.6), and (iii) the motions of mantle plumes that rely on backward advection of present mantle density structures. Incorporating data from hotspot tracks formed on different plates into a common reference frame requires estimates of relative plate motion. That is achieved by reconstructing coeval locations from all the tracks that are present at a certain age relative to a selected 'anchor' plate, which is most commonly South Africa (Unit 701, Chapter 3). A global absolute plate motion model is therefore made in such a way that all the tracks were on the southern African Plate (using plate circuits, Fig. 2.4) and then averaged to define a global moving hotspot reference frame (GMHRF).

The GMHRF of Steinberger et al. (2004) was based on four hotspot tracks, two in the Pacific (Hawaiian and Louisville), one in the South Atlantic (Tristan), and the fourth in the Indian Ocean (Réunion). All those hotspots probably initiated as LIPs (catastrophic melting of the upper mantle) at around 125–120 Ma (Ontong Java: Louisville), 134 Ma (Paraná–Etendeka: Tristan), and 65 Ma (Deccan: Réunion). Indo-Atlantic Plate circuits are quite robust but relating the Pacific Plate to the Indo-Atlantic system is not straightforward. The Steinberger et al. (2004) model of hotspot motion predicted a southward motion (up to a few cm/year) of the Hawaii Hotspot, and in combination with a plate motion chain that connects Africa and the Pacific via East Antarctica and Marie Byrd Land (West Antarctica) allowed a fit of hotspot tracks globally for times after the age of the Hawaiian–Emperor bend. In this model, no motion occurred between East Antarctica and Marie Byrd Land prior to 43.8 Ma (model A in Fig. 2.4b). Before 43.8 Ma, an east west misfit between predicted and observed Hawaiian hotspot tracks remains (Fig. 2.5a). Steinberger et al. (2004) thus explored alternative plate circuits linking Africa and the Pacific via East Antarctica Australia–Lord Howe Rise in older times (Model B, Fig. 2.4c), and with this model they were able to achieve a reasonable fit to hotspot tracks globally back to around 65 Ma. Prior to that, a notable misfit between predicted and observed Hawaiian tracks remains (Fig. 2.5a).

The GMHRF of Torsvik et al. (2008b) also used the model B plate motion chain of Steinberger et al. (2004), but relative plate motions are slightly different and the South Africa *versus* East Antarctica and Australia *versus* Lord Howe Rise rotations were smoothed. The transition between models A and B was also smoothed. By doing that, at 75 Ma (Campanian), the difference between observed and predicted

Fig. 2.4 (*cont.*) centre of the plate circuit tree, thus limiting error propagation. Abbreviations in our 200 Myr reconstruction keeping Africa fixed: SIB, Siberia; EUR, Europe; GRE, Greenland; NAM, North America; IBE, Iberia; NWAFR, North-West Africa; NEAFR, North-East Africa; SAFR, South Africa; AMC, Amazonia Craton; PAR, COL, Paraná, Colorado sub-plates; PAT, Patagonia sub-plate; IND, India; ARA, Arabia; MAD, Madagascar; EANT, East Antarctica; AUS, Australia; Th, Tethyan Himalaya. Once peri-Gondwanan terranes (dark greenish) and not part of Pangea include Ta (Taurides, Turkey), Po (Pontides, Turkey), Sa (Sanand, Iran), Lu (Lut, Iran), Al (Alborz, Iran), Af (Afghanistan), Qi (Qiantang, North Tibet), Lh (Lhasa, South Tibet) and SibM (Sibumasu). China block not part of Pangea (separated from Asia by the Mongol–Okhotsk Ocean) includes A (Annamia), SC (South China), NC (North China), and AM (Amuria, Central Mongolia). We also show two different relative plate circuit models between Indo-Atlantic (Africa) and Pacific hotspots before the Middle Eocene (Chron 20, 43 Ma). After Chron 20, models A and B follow the same plate motion chain through East Antarctica and Marie Byrd Land. The models were originally named model 1 and 2 (Steinberger et al., 2004). (b) and (c) Late Cretaceous (Maastrichtian) South Pacific reconstructions, the standard model A and the alternative plate chain model B, which link Africa and the Pacific via East Antarctica, Australia, and the Lord Howe Rise (LHR). For the South-West Pacific Plate motion chain, model B predicts intra-Antarctic motion prior to 43.8 Ma with extension in the Ross Sea area, whereas model A does not involve movements between East and West Antarctica before 43.8 Ma. The large arrows show paths of plate motion chains, thick stippled lines are divergent plate boundaries with sea-floor spreading, and dotted lines are conditional intra-continental plate boundaries necessary to accommodate the two different plate circuit models. The standard model A demonstrates a New Zealand misfit whilst model B requires about 300 km extension in the Ross Sea. CHL, Challenger Plateau; CAM, Campbell Plateau; MBL, Marie Byrd Land.

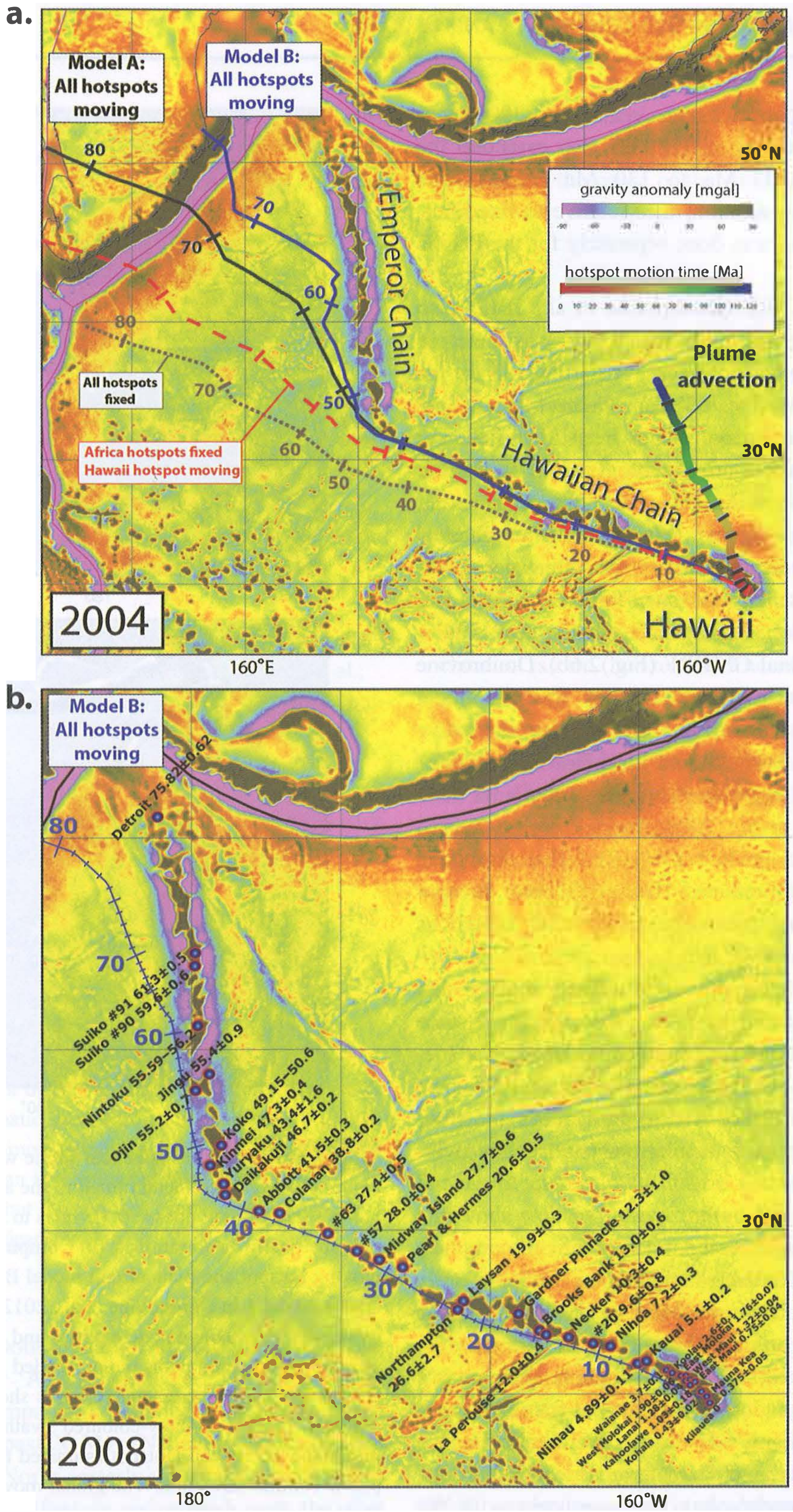

Fig. 2.5 (a) Dotted line: Computed fixed hotspot track for Hawaii in a reference frame based on fixed African (Tristan and Réunion) hotspots and plate chain model A (Fig. 2.4b). Dashed line: Same reference frame, but Hawaiian hotspot motion (due to plume advection, as shown in the figure) considered. Neither mimics the trend of the Emperor–Hawaii Chain. The black line (track computed in a reference frame that best fits four hotspot tracks – Hawaii, Louisville, Tristan and Réunion – and considers computed hotspot motion using plate chain model A) partly mimics the bend but plots west of the Emperor Chain. A model B plate chain (blue line) clearly improves the fit to the Emperor Chain and captures the Emperor–Hawaii Chain for the past 65 Myr quite well. (b) Predicted tracks for the Hawaii Hotspot in the global moving hotspot reference frame of Torsvik et al. (2008b). Hawaiian hotspot motion is the same as in (a) with model B plate circuits, but the transition between model A and B (46.3–43.8 Ma) and the plate circuits between East Antarctica–South Africa and Australia–Lord Howe Rise are smoothed compared with (a).

Hawaii–Emperor hotspot tracks was reduced to 300 km or less (Fig. 2.5b). Torsvik et al. (2008b) also extended the GMHRF from about 83 Ma to 130 Ma (Africa) and 150 Ma (Pacific), using rotation rates relative to fixed hotspots, but the extension was done separately for the Pacific and Africa.

A more recent GMHRF (Doubrovine et al., 2012) also included the New England hotspot track and was therefore based on a total of five hotspot tracks. A starting LIP for the New England Hotspot (located near Great Meteor Seamount, south of the Azores) has not been identified, but the New England track started with Triassic kimberlite intrusions in north-eastern America (e.g. Zurevinski et al,, 2011). Individual tracks were resampled with spherical splines (Fig. 2.6a), errors were assigned to track locations, a spherical regression and goodness of fit test was included, and an iterative model convergence scheme was implemented to derive the final GMHRF (Fig. 2.6b). Doubrovine et al. (2012) also tested fixed hotspot frames, model A *versus* B plate chains as in Fig. 2.5a and also alternative plate circuits between Australia and Lord Howe Rise. They concluded that model B (with Australia–Lord Howe Rise fits as in Steinberger et al., 2004; Torsvik et al., 2008b) produced the statistically best GMHRF. The difference between observed and predicted Hawaii Emperor hotspot tracks is much reduced compared with earlier GMHRFs (compare Figs. 2.5 and 2.6).

The GMHRF of Doubrovine et al. (2012) showed that Africa has been dominated by northward movement since the Cretaceous and the net longitude component for a specific location in Africa (15° N, 20° E) is less than 10° for the past 120 Myr (Fig. 2.8a). For Africa, the Doubrovine et al. (2012) GMHRF shows gross similarities (statistically overlapping) with that of Torsvik et al. (2008c), except for 60 and 70 Ma. For the past 100 million years we also show the movement of Africa based on the Indo-Atlantic moving hotspot (O'Neill et al., 2005; the 'rotation motor' of Seton et al., 2012) and 'slab-fitting' (van der Meer et al., 2010) frames. These frames are compatible with the GMHRFs for only the past 40 million years; the slab-fitted (subduction) frame is a direct derivation of the Indo-Atlantic hotspot frame in which longitudes of all the Earth's continents were calibrated so that the location of subducted material (identified in the mantle by seismic tomography) was consistent with the plate tectonic model. The subduction frame consistently predicts more westerly longitudes (Fig. 2.8a) than any other reference frame, and is to a large extent based on positioning the Farallon–Mexican–Caribbean South American slabs near (below) the Andean-type continental margin of the Americas.

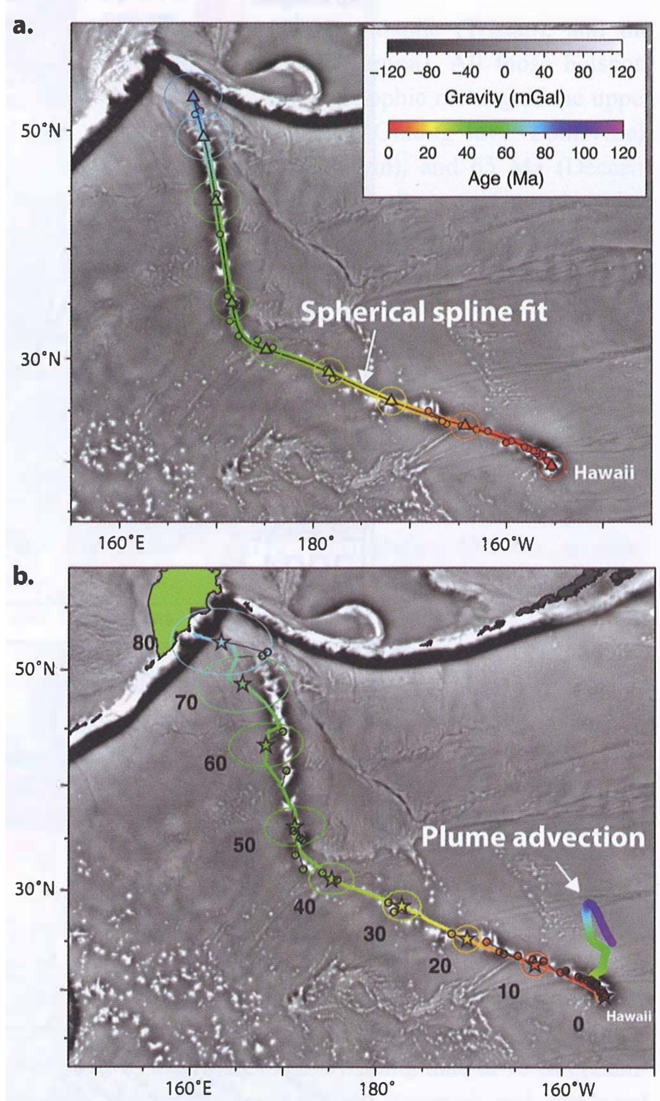

Fig. 2.6 (a) Smoothed spherical spline with 95% uncertainty circles (10 Myr increments) fitted to the age data for the Hawaiian hotspot track. Small dots with tie-lines to the spline are locations of radiometrically dated samples. (b) Computed motion and track for a moving hotspot and plate circuit model B (with Australian plate circuit model 1 in Doubrovine et al., 2012). Model track calculated by combining absolute plate motions and hotspot motions is shown as rainbow-coloured paths (colour-coded according to age) with crosses at 10 Myr increments (ellipses show the 95% uncertainty regions). Thicker rainbow-coloured swaths represent the surface motion of the Hawaii Hotspot estimated from numerical models of plume conduit advection. The global moving hotspot model of Doubrovine et al. (2012) was calculated from five hotspot tracks, four as in Fig. 2.5, and also the New England seamount chain. In modelling the Réunion hotspot track, Doubrovine et al. (2012) excluded Site 707 (erupted close to a ridge and about 500 km from the Réunion plume conduit) and Chagos (Site 713) was modelled to belong to the African (and not Indian) Plate at ~50 Ma (Torsvik et al., 2013).

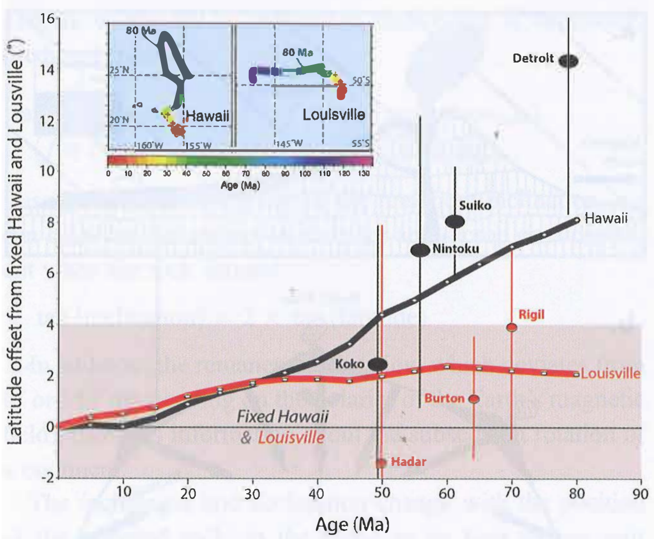

Fig. 2.7 Palaeomagnetically derived latitudes for seamounts along the Emperor (Detroit, Suiko, Nintoku, and Koko; Tarduno et al., 2003; Doubrovine & Tarduno, 2004) and Louisville Chains (Rigil, Burton, and Hadar; Koppers et al., 2012). Latitudes are shown as latitude offsets from zero (observed latitude minus latitude of Hawaii and Louisville) and compared with latitudinal estimates of plume advection (Doubrovine et al., 2012). For a system with fixed plumes (and no true polar wander) all the latitudes should be on the zero line, i.e. same latitude as Hawaii and Louisville today. Inset diagrams show the modelled surface motion (colour coded) of the Hawaii and Louisville hotspots back to 120 Ma. Hawaii is characterised by southward motion for the past 100 Myr whilst Louisville is dominated by eastward motion. This is also clearly reflected by palaeomagnetic data where the Emperor seamounts show large latitude deviations whereas latitudes of the Louisville seamounts are within error of the present-day location of Louisville (but show a small systematic southward component from Rigil to Hadar). The Emperor seamounts indicate more advection of the Hawaii plume conduit than that estimated from numerical modelling (Chapter 14), but the latitudes estimated for Koko, Nintoku, and Suiko are clearly within errors.

The GMHRF of Doubrovine et al. (2012) shows that absolute velocities for 'Africa' peaked at 5.5 cm/yr in the Upper Cretaceous (Campanian), declined during most of the Cenozoic, and for the past 20 Myr (Neogene) have averaged 1.4 cm/yr (Fig. 2.8b). North-easterly directed (as seen today) motion of the African Plate is recognised over the past 40 Myr. Absolute rotations for the remaining plates are calculated by adding the relative plate motions to the absolute rotations of southern Africa. Two examples of this are shown in Fig. 2.8c: Europe (Oslo) has not moved much in the last 120 Myr and has been extremely stable for the past 30 Myr, with absolute velocities below 1.5 cm/yr (Fig. 2.8b). Conversely, North America has moved about 50° westwards in the past 120 Myr; the dominant longitude change (Fig. 2.8c) is the cause of the so-called Cretaceous apparent polar wander 'still-stand' in North America (Torsvik et al., 2008b).

Palaeomagnetism

The Earth's magnetic field is described by its inclination (angle with respect to the local horizontal plane), declination (angle with respect to the local north south meridian), and field strength. The inclination of the Earth's magnetic field varies systematically with latitude (Fig. 2.9), which is of prime significance for palaeomagnetic reconstructions. For example, at the north magnetic pole, the inclination of the field is +90° (vertically down), and at the Equator the field inclination is zero (horizontal). The magnetic north and south poles normally differ from the geographical north and south poles because the magnetic axis is inclined relative to the geographical (rotation) axis (today ~11.5°). The magnetic axis, however, is slowly precessing around the geographical axis and, over a period of a few thousand years, it is probable that the averaged magnetic poles have corresponded reasonably well with the geographical poles. That is known as the geocentric axial dipole (GAD) hypothesis. We can therefore imagine that a magnetic dipole is placed at the centre of the Earth and aligned with the Earth's rotation axis (Fig. 2.9b).

There are various ways in which a rock can acquire a remanent (permanent) magnetisation parallel to the Earth's magnetic field at a given location (Fig. 2.9a), and the cooling of a basaltic lava flow from high temperature is an example. The most important magnetic mineral in basaltic rocks is titanomagnetite with maximum Curie temperatures (i.e. temperature above which a magnetic material loses its magnetism because of thermal agitation) near 580 °C (pure magnetite). During a basaltic volcanic eruption, the temperature of a lava is about 1,200 °C, but, when cooled below the Curie temperature, the magnetic minerals acquire a *thermoremanent magnetisation* (TRM) aligned with the Earth's magnetic field (Fig. 2.9b). The declination, inclination, and magnetisation intensity (proportional to the strength of the field), can be measured in the laboratory. In a comparable way, during the deposition of sediments, magnetic mineral grains settle on average in the direction of the Earth's magnetic field and a *detrital remanent magnetisation* (DRM) is acquired. DRMs, however, are commonly associated with inclination shallowing errors, which are latitude dependent (Tauxe & Kent, 2004; Kent & Tauxe, 2005; Kodama, 2009;

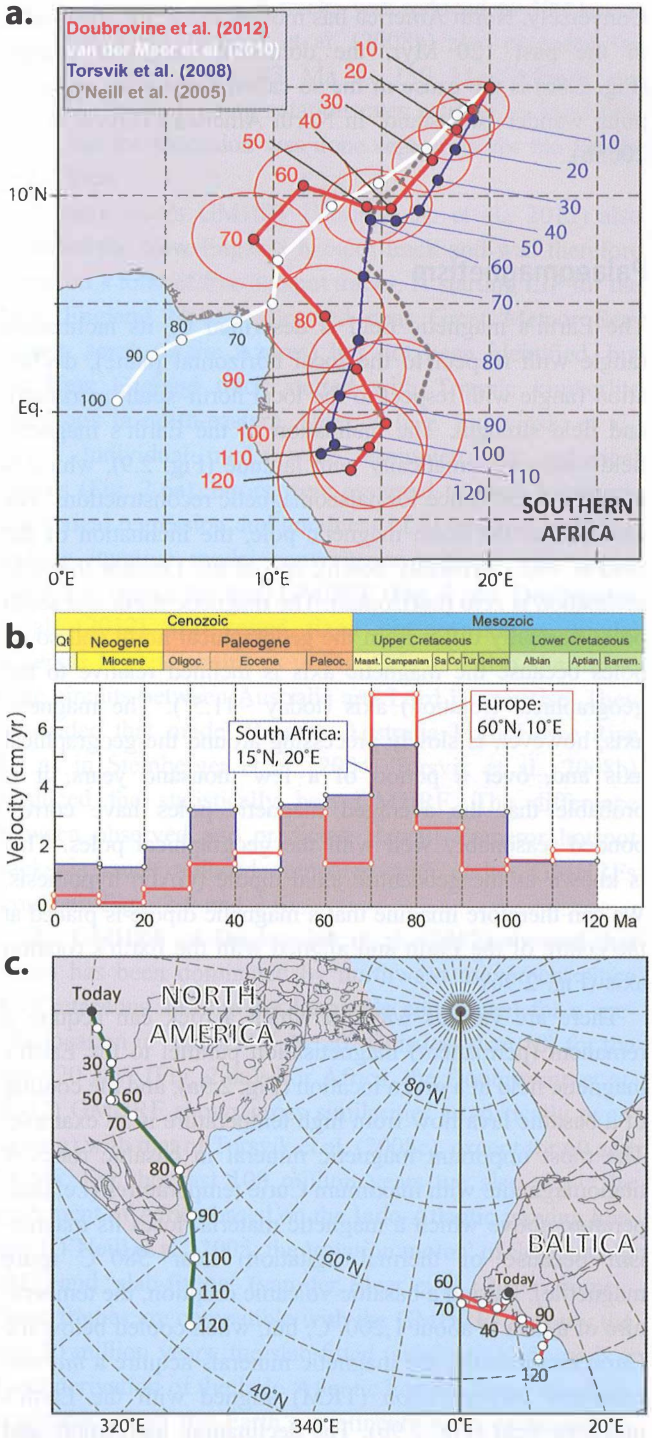

Fig. 2.8 (a) Africa motion (15° N, 20° E) in two different global hotspot reference frames (GMHRFs) at 10 Myr increments. Red dots and lines correspond to the GMHRF of Doubrovine et al. (2012). Blue is based on an earlier GMHRF by Torsvik et al. (2008b). For the Cretaceous (120–80 Ma) and the past 50 Myr, the two reference frames show gross similarities, but there are notable differences at 70 and 60 Ma. We also compare these GMHRFs with an Indo-Atlantic reference frame for the past 100 Myr (stippled

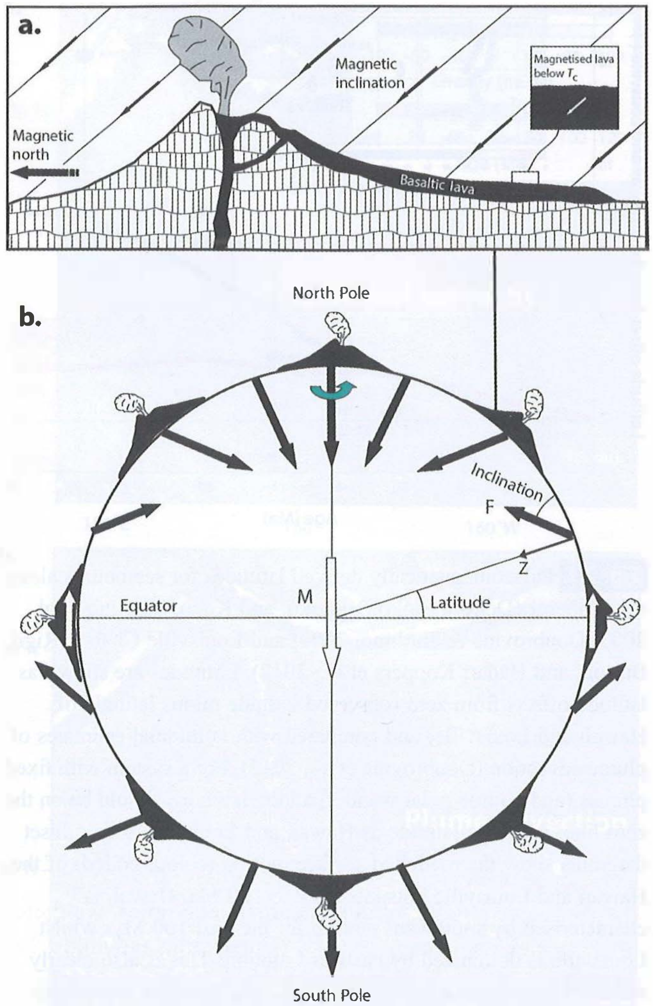

Fig. 2.9 (a) Example of acquisition of a thermoremanent magnetisation at intermediate northerly latitudes (acquired in a normal polarity field similar to today's). A lava will acquire a thermoremanent magnetisation upon cooling below the Curie temperature (T_C), and the inclination will parallel the inclination of the external field and have declination due north. (b) Field lines at the Earth's surface for a geocentric axial dipole. At the Equator the inclination is flat (zero), and at the north and south poles the inclination is vertical (+90° and −90° respectively). The inclination recorded in volcanoes formed on the Earth's surface is dependent on the latitude. Declinations in a normal polarity field, such as today's, should point to the north. Note that longitude cannot be determined because volcanoes erupted at different longitudes will always have the same inclination and declination.

Fig. 2.8 (*cont.*) brown line; O'Neill et al., 2005) and a slab-fitting frame (white thick lines; van der Meer et al., 2010) derived from the former (only longitude shifts). (b) Absolute velocities for a location in Africa and Europe (Oslo). (c) North America and Europe (Oslo) plate motion based on Doubrovine et al. (2012).

Torsvik et al., 2012). Inclination shallowing is commonly predicted from:

$$\tan(\text{inclination}_{\text{observed}}) = f \times \tan(\text{inclination}_{\text{field}})$$
$$(f \text{ is flattening factor; } f = 1, \text{no flattening})$$

Based on the measurement of the remanent inclination, we can calculate the ancient latitude for an outcrop on a continent when the rock formed:

$$\tan(\text{inclination}) = 2 \times \tan(\text{latitude})$$

In addition, the remanent declination, which deviates from 0° or 180° (depending on the polarity of the Earth's magnetic field), provides information about the subsequent rotation of a continent.

The inclination and declination change with the position of the sampled rock on the globe as its host terrane unit moves with time (Fig. 2.9b), but the direction of the magnetic pole of a GAD is independent of the locality at which the rock acquired its magnetisation. Thus it is practical to calculate pole positions so as to compare results from various sites and to provide objective data to underpin plate tectonic reconstructions. Ideally, as a time average, a palaeomagnetic pole (calculated from the declination, the inclination, and the geographical site location) for a newly formed rock will correspond to the geographical pole. If a continent moves later, the palaeomagnetic pole moves with the continent. To create a reconstruction with palaeomagnetic poles, we therefore have to calculate the rotation (Euler) pole and angle that will bring the palaeomagnetic pole back to the geographical north or south pole, and then rotate the continent by the same amount. In our example (Fig. 2.10a), a Late Permian palaeomagnetic pole from Oslo, Norway, will position Baltica at latitudes between 15° and 50° N, causing Oslo to have been located at 24° N. Therefore, because the current latitude of Oslo is 60° N, Baltica must have drifted northwards since the Permian.

Because its palaeolongitude is unknown from palaeomagnetic measurements alone, we can position Baltica at any longitude we wish, subject to other geological constraints. In addition to that, we cannot tell in old rocks whether a palaeomagnetic pole is a south or north pole. In Fig. 2.10a, we assumed that the pole was a north pole, but, if we used a south pole, Baltica would plot in the southern hemisphere but in a geographically inverted orientation (Fig. 2.10b). Hence, there is freedom to select north or south poles when producing reconstructions, placing the continent in an opposite hemisphere and rotated by 180°. The hemispheric choice is simple in this case, since Baltica had formed part of Pangea from 320 Ma, but in the deeper past it can be a problem.

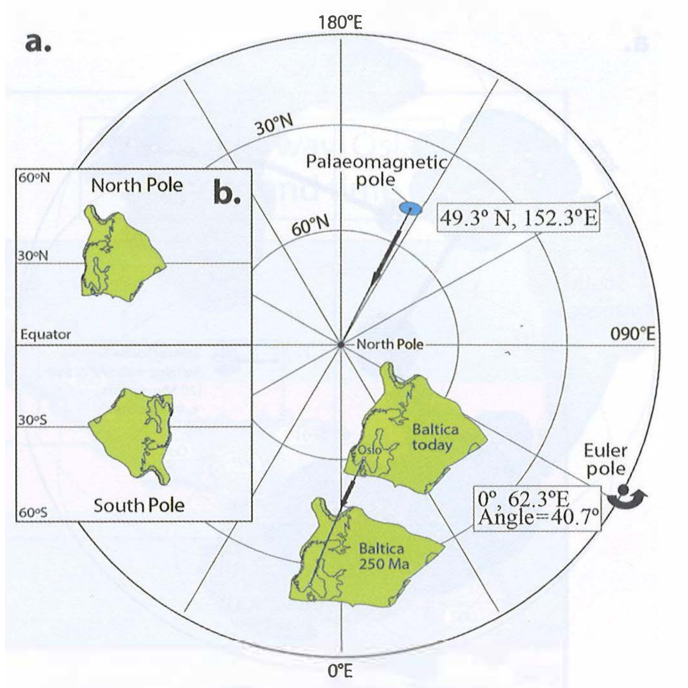

Fig. 2.10 (a) The reconstruction of a continent, in this diagram Baltica, is achieved as follows. Determine the Euler pole needed to rotate a palaeomagnetic pole (in this case a 250 Ma pole: 49.3° N, 152.3° E from Oslo, Norway) to the geographical North Pole (we calculate 0°, 62.3° E and a rotation of 40.7°). This Euler pole is then used to rotate the continent by the same amount. Thus Baltica today is rotated back about this pole to the position it occupied in Late Permian times at 250 Ma. (b) In (a), we assumed that the palaeomagnetic pole was a north pole. If we assume that it was a south pole, then the continent will have been situated in the opposite hemisphere, and geographically inverted (after Torsvik & Cocks, 2005).

Apparent Polar Wander (APW) Paths

Palaeomagnetic results can be expressed in terms of palaeopoles that are calculated using the GAD model. Those palaeopoles can in turn be used to construct APW paths. In this way, the motion of the polar axis relative to the continent (held fixed) is visualised. Many APW paths have been published for Baltica and its younger incarnations (Stable Europe) and the currently accepted path is shown in Fig. 2.11a (Torsvik et al., 2012). By keeping Baltica/Europe fixed, mean south poles for the Cambrian are located in Arctic Siberia (not shown in diagram), followed by a drift of the pole over Arabia and Central Africa in the Ordovician to the Atlantic off the north-east corner of Brazil in the Silurian–Devonian cusp. Subsequent southward movement brought the south pole near

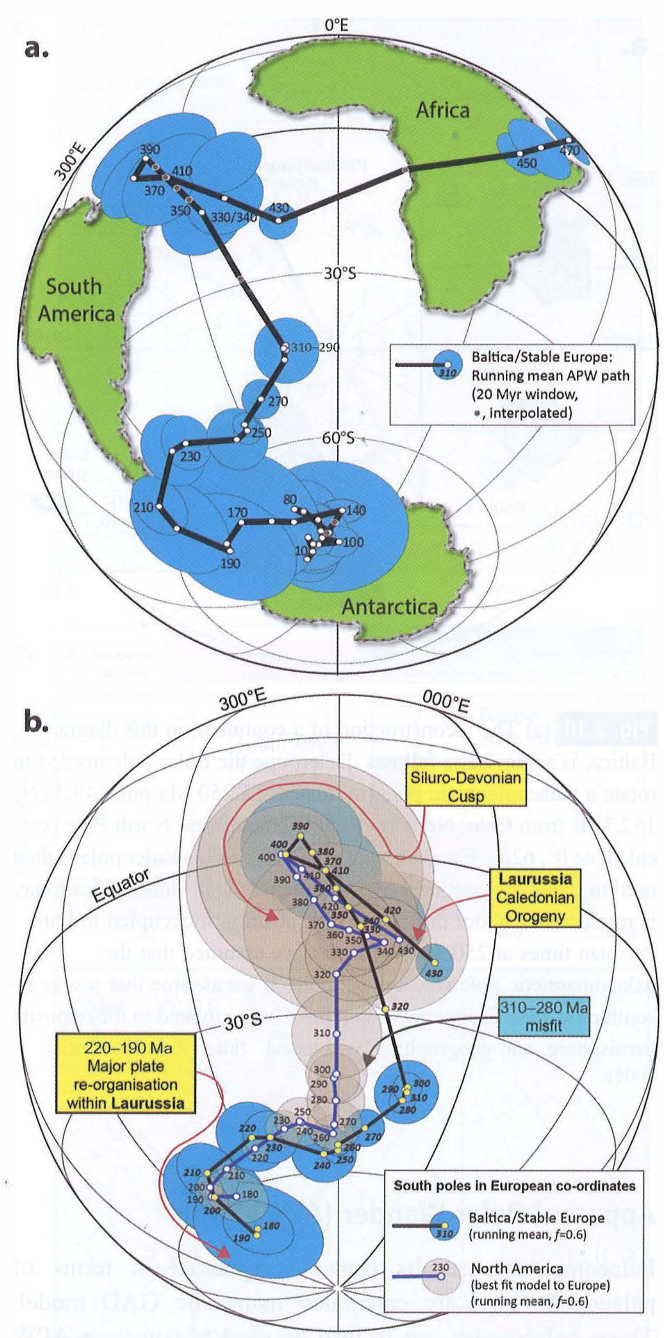

Fig. 2.11 (a) Running mean APW path (20 Myr window) for Baltica/Stable Europe shown with 95% confidence ovals at 10 Myr intervals. The APW path shows the movement of the south pole relative a fixed Baltica/Europe (grey shaded circles are interpolated). (b) Best fit of North American and Baltic/Stable Europe APW paths (running means) from 430 Ma (formation of Laurussia) to 190 Ma. Late Carboniferous Early Permian poles (310 280 Ma) have been excluded in the fitting procedure, and between 220 and 190 Ma the Euler fit changes from 78.7° N, 161.9° E (angle = −31.0°) to 69° N, 154.8° E (angle = −23.6°). Palaeomagnetic input poles listed in Torsvik et al. (2012).

Patagonia in the Triassic, after which the pole remained close to Antarctica in the Jurassic.

From palaeomagnetic data, we calculate APW rates, the latitude for a specific location through time, north south latitudes (longitude unknown), and the speed and change in angular rotation of a continent (Fig. 2.12). In our Baltica example, Oslo has drifted northwards from 60° S to 60° N during the Phanerozoic. North–south velocities were notably high (about 12 cm/yr) during the Late Ordovician–Early Silurian (just prior to and during collision with Laurentia and the subsequent formation of Laurussia), and the Late Carboniferous (Pangea assembly). Angular rotations peaked in the Early Ordovician, when Baltica was rotating counter-clockwise at rates of up to 5° /Myr.

In Fig. 2.12a we show an example of reconstructing Baltica's changing position over the past 500 million years based on the palaeomagnetic data (Fig. 2.11a). In Late Cambrian and Early Ordovician times (500 and 470 Ma reconstructions) Baltica was strongly rotated (compared with today) and was located in the southern hemisphere. Since Late Devonian times, Baltica has largely undergone northward drift. The westerly longitudinal movement of Baltica (with decreasing time in Fig. 2.12a) is entirely subjective, but there is an analytical trick that can constrain longitude semi-quantitatively for the times after Pangea formed at about 300 Ma. But that trick requires that we identify the continent that has moved the least in longitude, and, after reconstructing that particular continent, all the other continents must be reconstructed relative to it in order to minimise longitudinal uncertainty. We therefore need to build a global APW path through the continent's history. Taking relative plate motions into account, palaeomagnetic data from all the major continents can be combined in a global APW path. However, the choice of an appropriate reference plate for that global APW is critical. Judicious selection of that reference plate results in reduced longitudinal uncertainty in palaeogeographical reconstructions. The 'zero-longitude' Africa approach (Burke & Torsvik, 2004; Torsvik et al., 2008c) makes use of the observation that Africa has remained the continent that has moved least in longitude since the breakup of Pangea. To build a global APW path (GAPWaP) we must first compile all reliable palaeomagnetic data worldwide (from stable cratons) and rotate all the raw poles to South Africa co-ordinates to calculate a running mean GAPWaP (alternatively use spherical splines). Next we calculate Euler poles from the GAPWaP to reconstruct South Africa, and then the remaining plates are reconstructed with plate chains relative to South

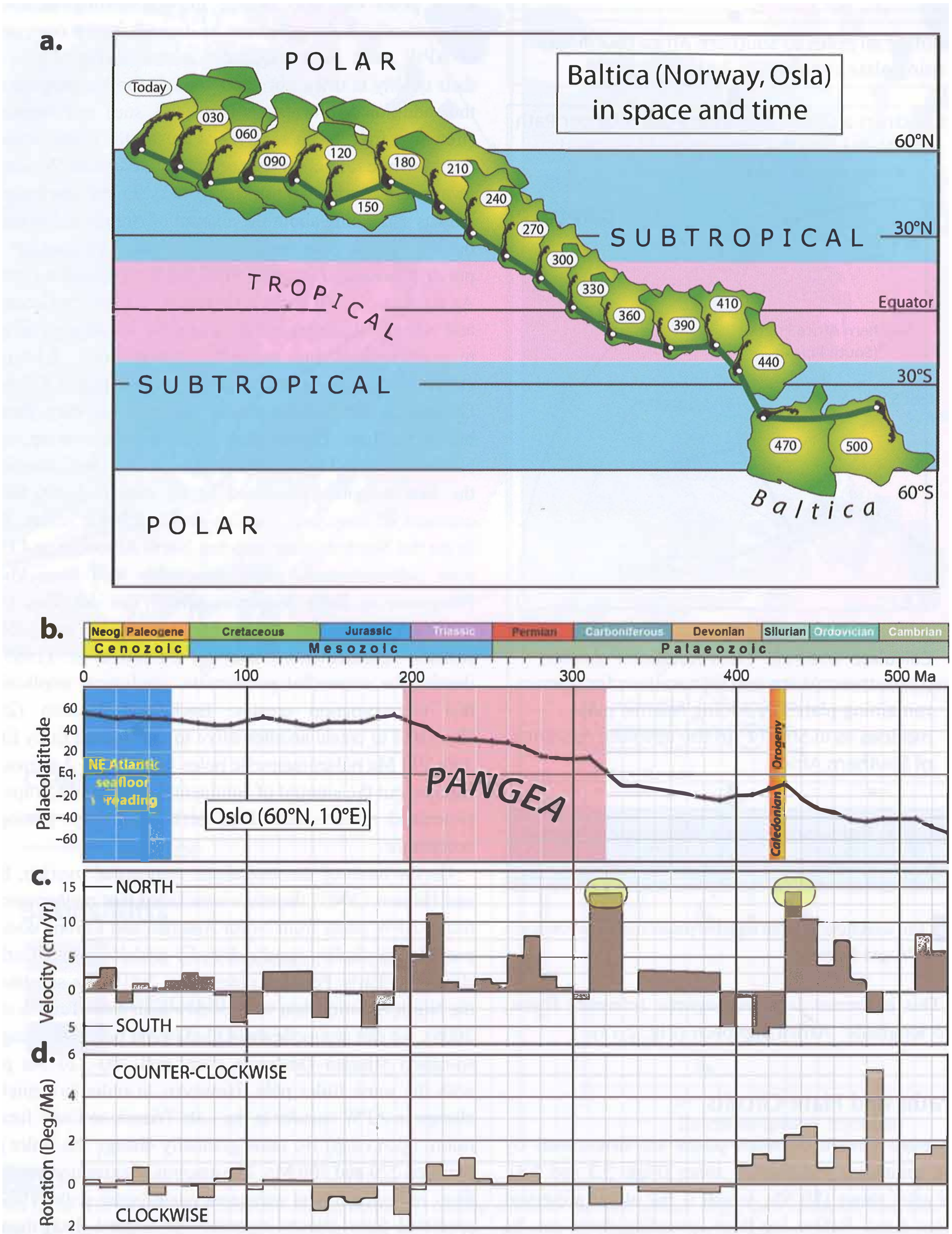

Fig. 2.12 (a) The drift history for Baltica (Oslo) at 30 Myr intervals based on the APW path in Fig. 2.11a. We also indicate the collision with Laurentia (Caledonian Orogeny), the time interval Pangea existed, and sea-floor spreading in the north-east Atlantic when Baltica separated from Laurentia (Greenland), which is still ongoing. (b) Palaeolatitudes for Oslo in 10 Myr intervals. (c) Palaeolatitudes for Oslo separated into northward and southward motion (minimum velocities since palaeolongitude change are 'unknown'). (d) Rotation rate of Oslo.

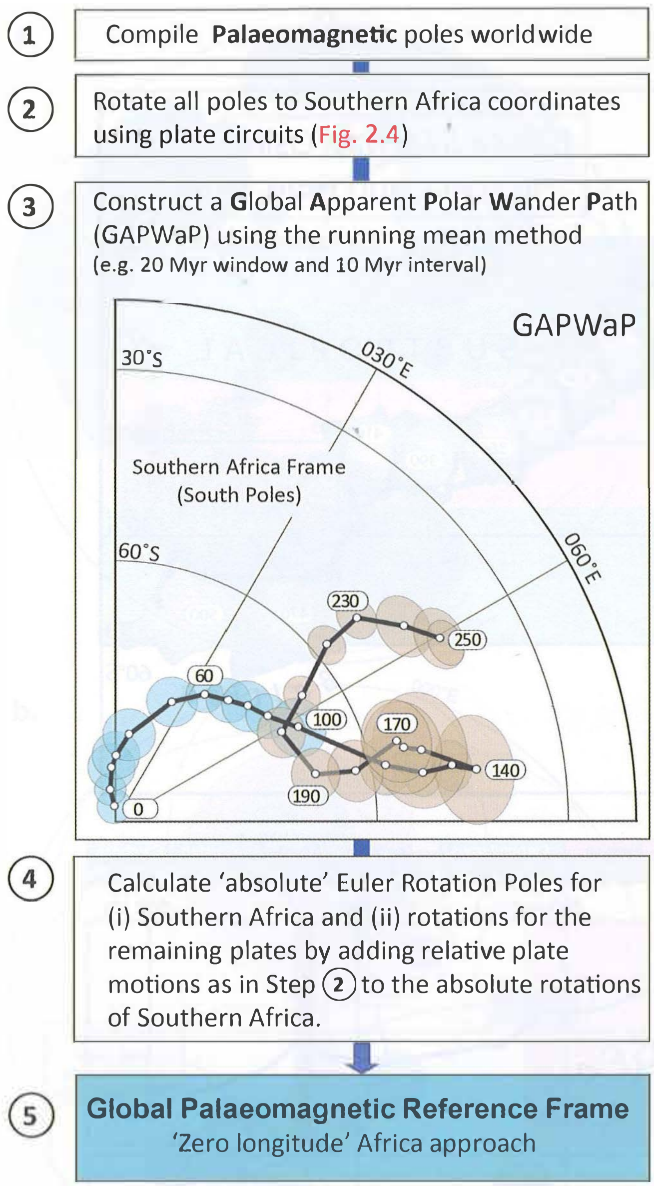

Fig. 2.13 The workflow to build a global palaeomagnetic reference frame since Pangea formed.

Africa. This is termed a palaeomagnetic reference frame, the 'zero longitude' Africa approach (Fig. 2.13).

APW Paths and Plate Circuits

Relative plate circuits between plates are determined by magnetic anomalies and fracture zones (Figs. 2.3 and 2.4), but only after about 180 Ma, which is the oldest preserved *in situ* sea floor. Before sea-floor spreading there can be hundreds of kilometres of stretching of the continental crust (here referred to as pre-drift extension) and therefore plate fits before breakup should be much tighter. As Euler poles and their angles change during sea-floor spreading, pre-drift Euler poles can also change through geological history. Theoretically, Euler poles can be derived from a comparison of APW paths from conjugate continents (Fig. 2.11b), but their quality is often not good enough for this purpose, and thus additional information is needed, such as estimates of stretching from basin analysis or crustal thickness estimates from seismic refraction data or gravity inversion. We assume an average continental thickness of say 35 km: anything less tells us something about the amount of stretching but not the timing. But on passive margins we normally consider that pre-drift extension stopped when sea-floor spreading started. As an example, we show a very tight fit between Greenland and Norway (Europe) in Fig. 2.14b. At 55 Ma and just prior to sea-floor spreading in the NE Atlantic (Fig. 2.14a), the current continent ocean boundary transitions (COBs) for Greenland and Europe almost coincide (as they should), but in the Late Triassic they show a huge overlap, up to almost 400 km (Fig. 2.14b). Bullard et al. (1965) developed the first computer-generated fit by matching 500-fathom contours of conjugate margins in the Atlantic realm. Their fit for the North Atlantic matches North American and European palaeomagnetic poles reasonably well from Middle Palaeozoic to Early Mesozoic times (Van der Voo, 1993; Torsvik et al., 1996; 2012). For that reason, many North Atlantic reconstructions use the Bullard et al. (1965) fit despite the somewhat problematic geological implications this reconstruction creates. Beck and Housen (2003) attempted to create an alternative to the Bullard fit by fitting 300–200 Ma palaeomagnetic poles from North America and Europe, but the amount of continental overlap of Europe and Greenland (over 1000 km) is beyond any geological acceptance.

On the basis of this unrealistic continental overlap, Beck and Housen (2003) therefore concluded that mathematically fitting APW paths from North America and Europe does not provide satisfactory results. But, by excluding Late Carboniferous to Early Permian poles (Fig. 2.11b), or substituting the North America data with Gondwanan data (Torsvik et al., 2006), we can reconcile the 430–330 Ma poles (defining the so-called Silurian–Devonian cusp) and 290–220 Ma poles with the same Euler pole. However, in order to depict the change in APW wander in the Late Triassic to Early Jurassic (more open cusp) we must gradually change the Euler pole between 220 and 190 Ma. The amount of extension predicted from our plate model compares much better with extension predicted from gravity inversion (or seismic data) than the classic Bullard fit (Fig. 2.14c). The implications of the plate model changeover between 220 and 190 Ma are discussed in Chapter 11.

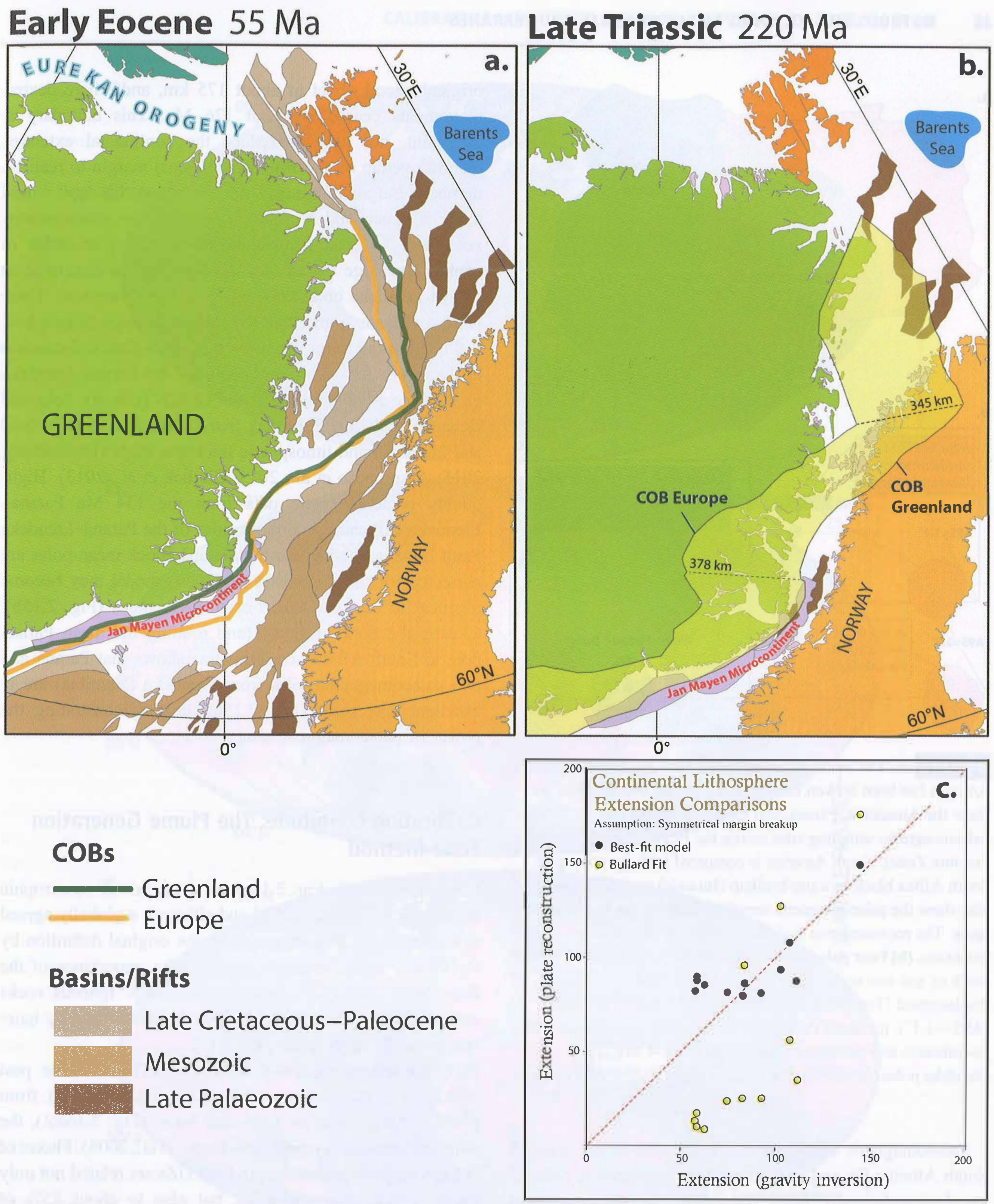

Fig. 2.14 Our plate model between Greenland and Norway (Europe) at 55 Ma (just prior to breakup and sea-floor spreading) and at around 220 Ma (a, b). The large COB (Continent–Ocean Boundary) overlap witnesses the total amount of pre-drift extension from then until breakup. We also show basins/rifts that developed from the Late Palaeozoic to the Paleocene. The Jan Mayen Microcontinent (now part of Eurasia) consisted of several distinct segments; the original size of these blocks at 220 Ma (b) was smaller than in present times because they are now composed of extended continental crust (18–20 km thick). (c) Comparing lithosphere extension derived from the plate model and gravity extension (crustal thickness) along 11 profiles between Greenland and Europe (Alvey et al., 2008). Symmetrical margin breakup is assumed and the values represent half of the continental overlaps in (b).

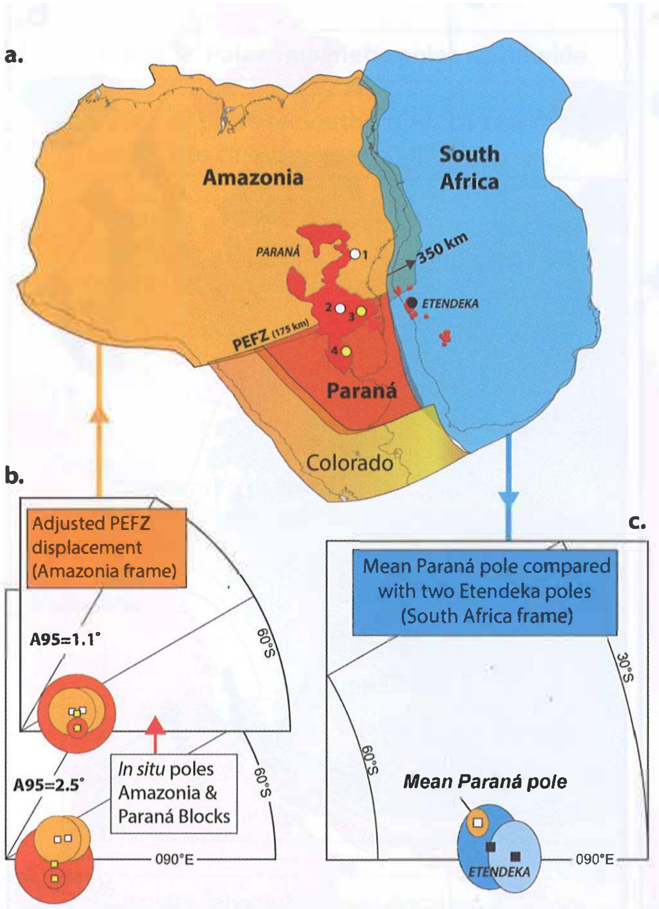

Fig. 2.15 (a) The South American intra-plate model where South America has been broken into several different blocks. Here we show the Amazonia, Paraná, and Colorado blocks and palaeomagnetic sampling sites across the PEFZ (Paraná–Etendeka Fracture Zone). South America is compared with the conjugate South Africa block in a pre-breakup (Jurassic) reconstruction. We also show the palaeomagnetic sampling location for the Etendeka lavas. The reconstruction includes 350 km of pre-breakup extension. (b) Four palaeomagnetic poles from the Paraná LIP; two south of and two north of the PEFZ. After adjusting for PEFZ displacement (Torsvik et al., 2009) the four poles fit perfectly (A95 = 1.1°). (c) Mean Paraná pole (N = 4) rotated to South Africa co-ordinates and compared with two recent 134 Ma Etendeka poles (Dodd et al., 2015; Owen-Smith et al., work in progress).

Palaeomagnetic data have also been used to test pre-drift South Atlantic fits and also intra-plate geometries in order to avoid unrealistically large continental overlaps (pre-drift extension) or gaps along the conjugate South Atlantic margins. Torsvik et al. (2009) divided South America into four main domains (Amazonia, Paraná, Colorado, and Patagonia). One of the most important boundaries (Fig. 2.15a) is between Amazonia and Paraná (Paraná Etendeka Fault Zone), modelled as a transtensional boundary with an original lateral offset of about 175 km, and where dextral movements ceased at about 126 Ma. This boundary is important, not only to reduce the continental extended margin overlap on the Brazilian (Santos) margin to realistic numbers, but also because extension along this fault would made it easier, and a preferred location, for plume-related volcanism to occur (upside-down drainage) in order to explain the large extent of Paraná volcanism compared to that of Etendeka on the conjugate margin (Namibia). There is no consensus from either the surface geology or geophysical data on the exact localisation of intra-plate deformation in the South American continent, but the Paraná–Etendeka Fault Zone is reçognised in the GOCE (Gravity field and Ocean Circulation Explorer) free air residual gravity field and in crustal and lithospheric thickness maps (Braitenberg, 2015; Assumpção et al., 2013; Chulick et al., 2013). High-quality palaeomagnetic data from the 134 Ma Paraná Etendeka LIP came from both sides of the Paraná–Etendeka Fault Zone, and when the two Paraná Block mean poles are corrected for the Torsvik et al. (2009) model they become identical to the two Amazonian Block poles (Fig. 2.15b). Closing the South Atlantic (and rotating the mean Paraná pole to South African co-ordinates) shows that Paraná and two palaeomagnetic poles from Etendeka (Namibia) are in excellent agreement (Fig. 2.15c), thus demonstrating the power of palaeomagnetic data.

Calibrating Longitude: The Plume Generation Zone Method

LIPs (Appendix 1, Fig. 2.16a) are the result of catastrophic melting in the upper mantle, and although a globally agreed definition of a LIP does not exist, the original definition by Coffin and Eldholm (1994) stressed the importance of the large areal extent of predominantly mafic igneous rocks emplaced in an intra-plate setting, and characterised by igneous pulses of short duration.

By reconstructing the positions of LIPs over the past 300 Myr, it has become clear that most originated from plumes at the edges of Tuzo and Jason (Fig. 2.16b,c), the plume generation zones (PGZs; Burke et al., 2008). Fluxes of hot and buoyant material from the PGZs are related not only to the emplacement of LIPs, but also to about 85% of kimberlite intrusions (Fig. 2.16c; Torsvik et al., 2010), and many hotspot volcanoes (Fig. 2.2b) such as at Hawaii (Pacific Ocean), Réunion (Indian Ocean), and Iceland (North Atlantic Ocean). But there are anomalies from this pattern; for example, Yellowstone in western North America. In fact, several hotspots, one LIP (Columbia River Basalt), and most

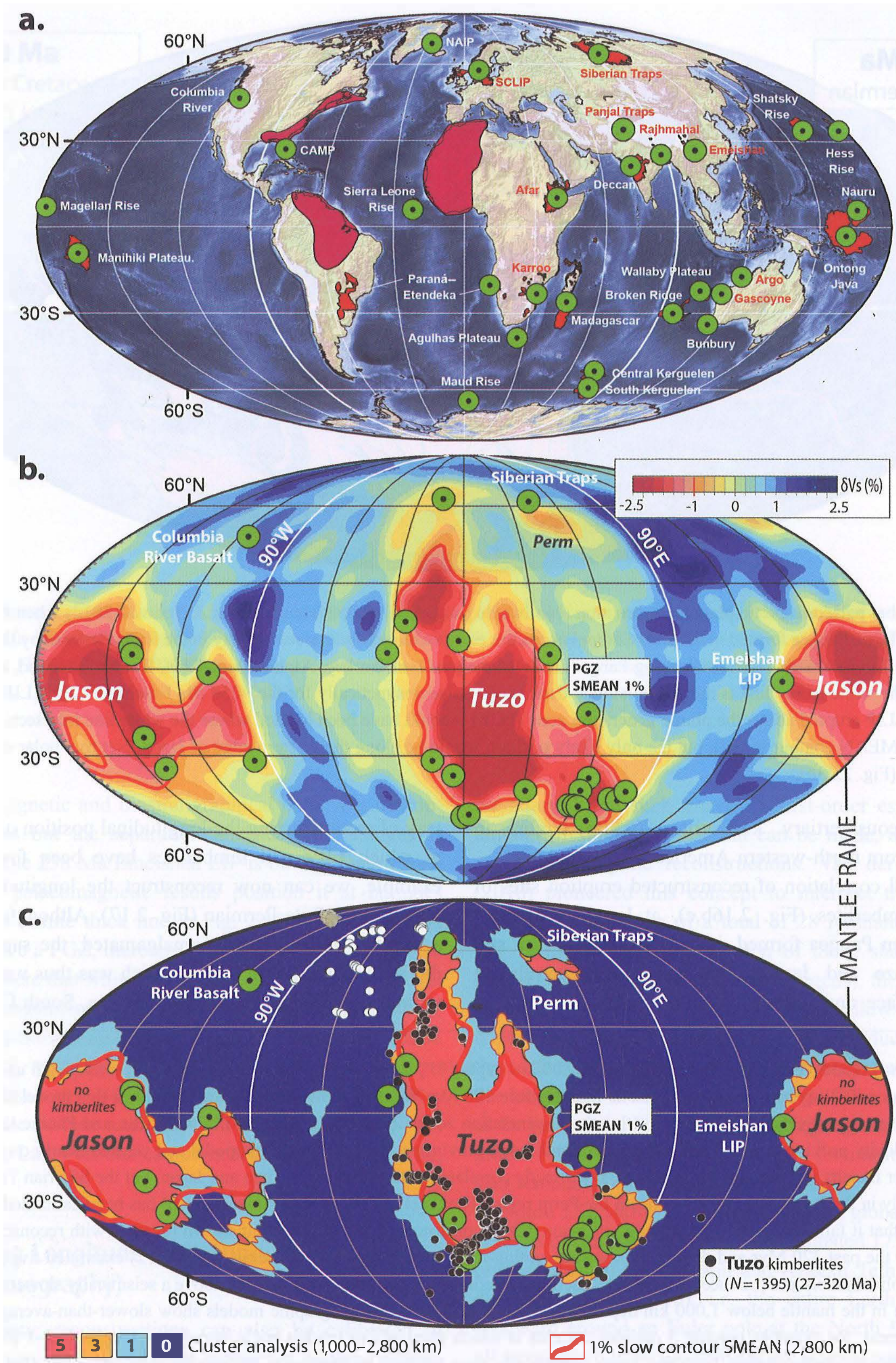

Fig. 2.16 (a) Large igneous provinces (LIPs, 15–297 Ma) and their estimated eruption centres. The Panjal Traps are allochthonous and thus associated with some reconstruction uncertainties in (b) and (c). The areal extent of the Central Atlantic Magmatic Province (CAMP) is liberal in the inclusion of all ~201 Ma basalts, sills and dykes. (b) The LIPs reconstructed and superimposed on the SMEAN tomographic

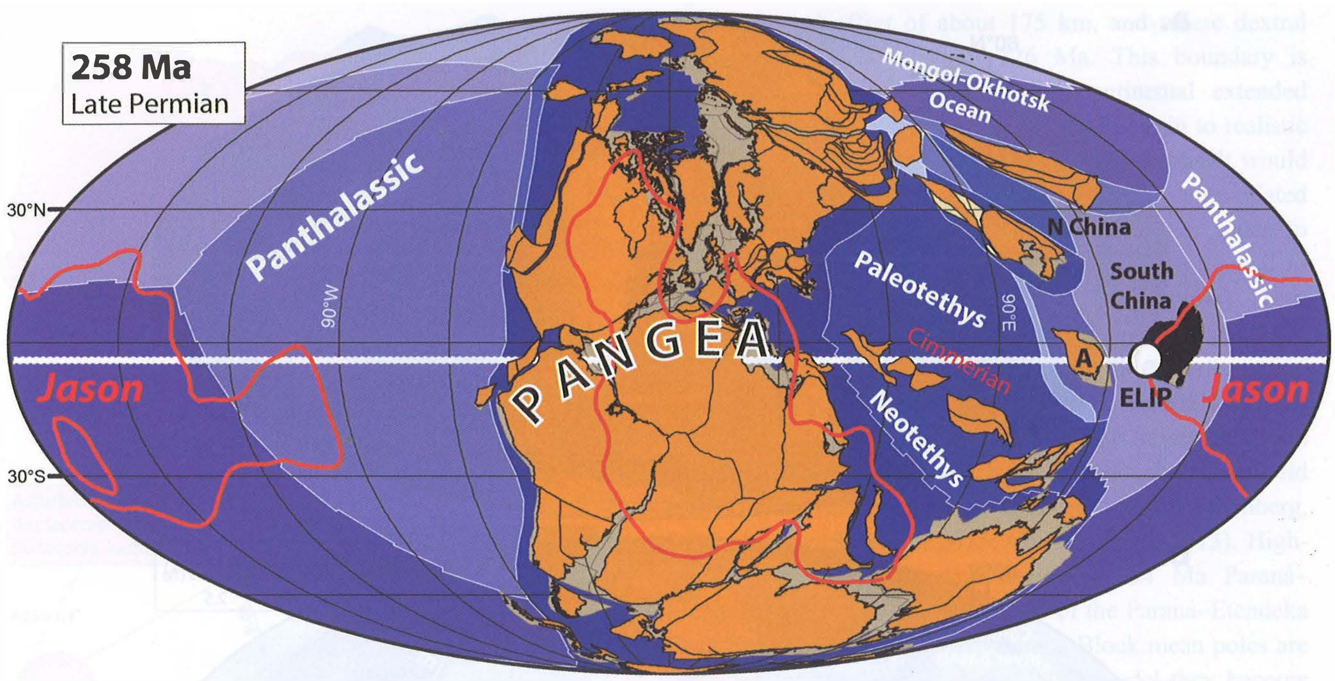

Fig. 2.17 Global palaeomagnetic plate reconstruction (Mollweide projection) at 258 Ma (Domeier & Torsvik, 2014) when Pangea was centred above Tuzo. Pangea formed in the Late Carboniferous but early breakup is witnessed already in the Early Permian by the opening of the Neotethys. The Cimmerian terranes leaving Pangea included parts of Iran, Turkey, Afghanistan, Tibet, Burma, Thailand, and Malaysia (Sibumasu). The white heavy line is the palaeolatitude determined palaeomagnetically for the ~258 Ma Emeishan LIP (ELIP) of South China. If the ELIP erupted above the plume generation zone (PGZ) it could have been located where the white line intersects a PGZ (here the 1% slow SMEAN contour in red), but the only likely position would be along the western edge of Jason. Net true polar wander at this time was zero (Fig. 2.23b).

Late Cretaceous/Tertiary kimberlites (white circles in Fig. 2.16c) from north-western America are anomalous.

The overall correlation of reconstructed eruption sites of LIPs and kimberlites (Fig. 2.16b,c), at least since about 300 Ma, when Pangea formed, indicates the long-term stability of Tuzo and Jason. That remarkable correlation between surface and mantle features provides an original way of reconstructing the longitudinal position of continents in which LIPs and kimberlites have been found. As an example, we can now reconstruct the longitude of South China in the Late Permian (Fig. 2.17). Although that was at a time when Pangea was amalgamated, the supercontinent did not include South China, which was thus without longitudinal constraints. In the Late Permian, South China, based

Fig. 2.16 *(cont.)* model (Becker & Boschi, 2002) at 2800 km depth (δV_s is the S-wave anomaly). LIPs are reconstructed using a moving hotspot frame or a TPW-corrected palaeomagnetic frame before 120 Ma. We also show the 1% slow contour in this model (SMEAN 1%) that we have used extensively as the proxy for the plume generation zones (Torsvik et al., 2006). The African and Pacific large low shear-wave velocity provinces (LLSVPs) are the Tuzo and Jason provinces; they are almost antipodal and centred nearly on the Equator. Columbia River Basalts and the Siberian Traps are not directly correlated with the edges of Tuzo and Jason, but the Siberian Traps overlie a smaller anomaly in the lowermost mantle beneath the Perm region (Lekic et al., 2012). The Emeishan LIP has been calibrated in longitude (Fig. 2.17) so that it falls above the western edge of Jason. (c) Reconstructed LIPs as in (b) but shown together with reconstructed kimberlites for the past 320 Myr and draped on a seismic voting-map in the lower mantle. Lekic et al. (2012) examined five global shear-wave tomographic models and produced a map that described whether a geographical location was above a seismically slower-than-average velocity region in the mantle below 1,000 km depth. Within contour 5, all five tomographic models show slower-than-average seismic velocities, whereas, for example, contour 3 outlines the area in which three of five models are in agreement. Contours 5–1 (only 5, 3, and 1 are shown here for clarity) define Tuzo and Jason (seismically slow regions) in addition to the smaller Perm anomaly. Contour 0 (blue) denotes faster regions in the lower mantle. The 1% slow SMEAN contour is shown for comparison. For the past 320 Myr, 80% of all reconstructed kimberlite locations (black dots) erupted near or over the Tuzo PGZ. The most 'anomalous' kimberlites (17%) are from Canada (white dots).

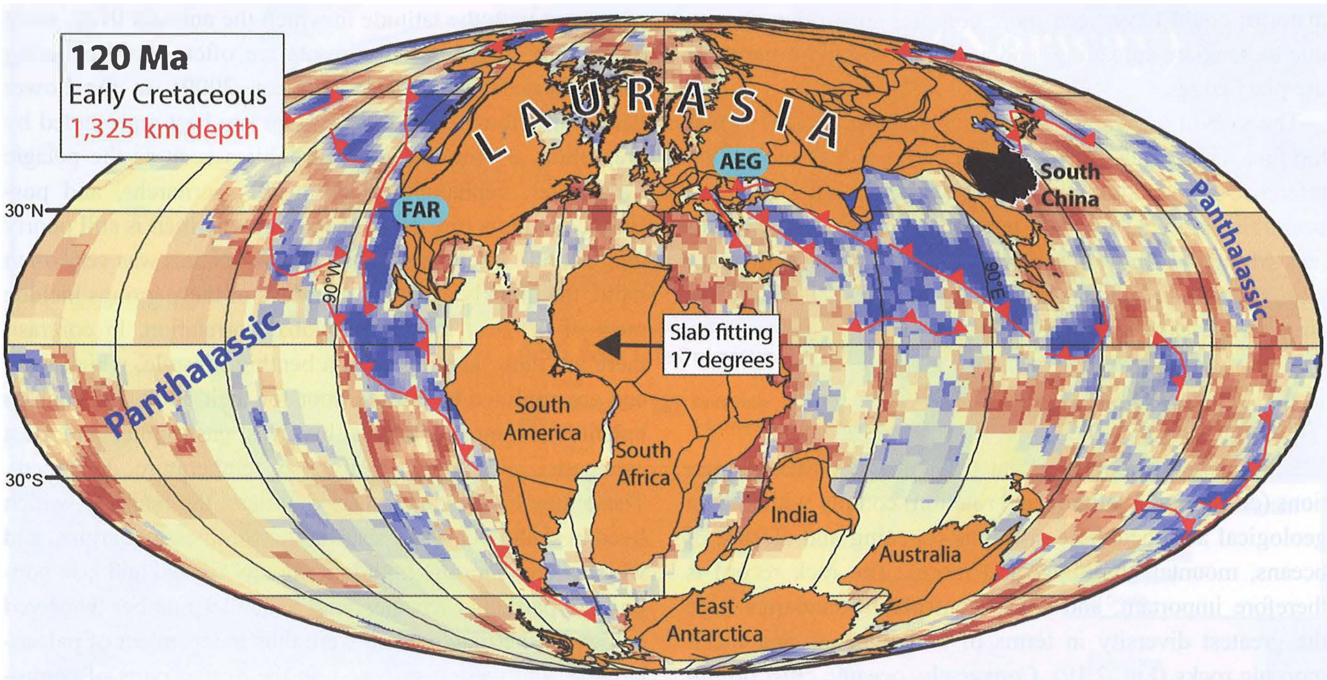

Fig. 2.18 Example of calibrating a 120 Ma reconstruction (based on palaeomagnetic data) in longitude (van der Meer et al., 2010). A reasonable fit was obtained between a 1,325 km tomographic depth-slice, Farallon and Aegean Tethys Ocean slabs when an absolute plate motion frame (Torsvik et al., 2010) was shifted 17° westwards. Interpreted subduction zones shown in red. AEG, Aegean slab; FAR, Farallon slab.

on palaeomagnetic and biostratigraphical data, was in tropical latitudes but the separation distance from Pangea is unknown. The 258 Ma Emeishan LIP is on the South China block, and palaeomagnetic results position it at latitudes around 4° S (white thick line in Fig. 2.17). If that LIP had erupted above a PGZ, there are several possible longitudinal locations where that white line of latitude crossed the PGZ at that time. Pangea covered two of those options (above Tuzo), leaving only the options related to Jason. The reconstruction in Fig. 2.17, with the Emeishan LIP above the western margin of Jason at ~134° E, is the only realistic alternative. Thus both the latitude and longitude (Appendix 1) of South China in the Late Permian can be established (Torsvik et al., 2008c).

Calibrating Longitude with Subducted Slabs (Tomography)

Palaeomagnetic reconstructions can also be calibrated in longitude using the positions of subducted material (slabs) which was subducted along convergent margins of the continents. Slabs can be observed in tomographic models at depths from the Earth's surface down to the core mantle boundary. From such images, a first-order estimate of the amount of subducted material can be made, and used as a constraint on plate reconstructions. Van der Meer et al. (2010) pioneered this concept to interpret the depth and timing of subduction of a total of 28 remnants of slabs in the mantle. Through correlation of those slabs with their geological record (fossil arcs and orogens), they determined a sinking rate of 12 ± 3 mm/yr, which allows surprisingly consistent global correlations of palaeo-subduction zones at the surface with seismic tomography images at depth. Thus the longitudes of ancient active margins can be constrained as far back as the Permian by adjusting a global plate motion model based on palaeomagnetic data for improved fits with slab remnants in the tomographic model.

Figure 2.18 shows an example where a global palaeomagnetic reconstruction at 120 Ma was adjusted 17° westward in order to best fit the Farallon and Aegean Tethys slabs (van der Meer et al., 2010), i.e. the entire Earth was rotated westward around an Euler pole at the North Pole. As with all reconstruction methods, there are several possible sources of error in the interpretation of these slab-fitting exercises, including the unknown slab dip, lower mantle thickening of slabs, and tomographic imaging. Furthermore, subduction histories could have been more complex than often shown, due to back-arc spreading, and accretion and deformation at the plate edges.

The slab-fitting model of van der Meer et al. (2010) was the first of its kind and can be dubbed a global subduction reference frame. Since then the ages of several slabs have been reinterpreted, there has been revision of ocean closures (e.g. Mongol–Okhotsk) and also development of more complex subduction models, e.g. along the western margin of North America (Fig. 13.6).

The Rock Record

It is of pivotal importance that palaeomagnetic reconstructions (constraining latitude and rotation) comply with known geological and tectonic constraints (opening and closure of oceans, mountain building, and more). The rock record is therefore important, and convergent plate boundaries have the greatest diversity in terms of both igneous and metamorphic rocks (Fig. 2.19). Conversely, oceanic crust originally formed at divergent plate boundaries can occasionally be obducted onto a continent (ophiolite), and dating that piece of old oceanic crust can tell an important story about ancient sea-floor spreading around that continent.

The Distribution of Fossils

Faunal and floral provinces have been identified at various times and places for the past two hundred years. Modern provinces are chiefly caused by differences in climate and temperature, which are in turn linked broadly to latitude; but also by the ability or inability of the biota to get across physical barriers, chiefly land (in the case of marine life) and seas (for terrestrial plants and animals). The identification of various faunal and floral groupings useful for palaeogeographical studies is particularly important during the Palaeozoic (Fig. 2.20a), older than any ocean floor that has been preserved.

The faunal principles have not changed since first set out by Cocks and Fortey (1982). Before any animal can be used, both its age and its individual ecology must be assessed correctly. The distribution of those animals with a planktonic, pelagic, or nektonic (swimming) lifestyle is controlled by oceanic currents and temperature, and thus, although the deposits in which their fossils are found usually form part of one or more of the terranes that we recognise as separate, those occurrences are of no significance when assessing the closeness or individuality of such terranes (Fig. 2.20b, c). Because the great majority of such animals are dependent on temperature, their occurrence may only be generally correlated with the latitude in which the animals lived, since warmer or cooler ocean currents are often found covering varied latitudes (Cocks & Verniers, 2000). In the Lower Palaeozoic, those planktonic groups are best represented by graptolites, a minority of the trilobites such as the pelagic *Carolinites*, cephalopods, chitinozoa, acritarchs, and possibly conodonts (the detailed ecology of which is still poorly understood). As the dispersal of these animals was very often rapid, the quickly evolving members of these groups include most of the best fossils for global correlation. In contrast, there are those animals with a benthic lifestyle, which were and are confined to the sea floor for their adult life, such as brachiopods, most trilobites, bivalves, gastropods, and most ostracods, and which were also temperature dependent. These may be divided into two groups: the majority, which lived in shallower-water seas on the continental margins, and which were therefore both latitudinally related and also confined to particular terranes; and a smaller number that lived below the thermocline and were thus independent of palaeolatitude, and were distributed on the deeper parts of continental shelves and on the ocean floors. It is the former, larger, group of benthic animals upon which we rely most strongly to provide the faunal support for terrane reconstructions. Cladistic analysis has been used to support some of the faunal distributions, but there are not enough truly robust trees for palaeobiogeographical use, and there are few such data from the Lower Palaeozoic. Despite the fact that the adult brachiopods and most trilobites were confined to relatively small sites, their larval stage was planktonic for shorter or longer periods and thus the genera dispersed as time progressed.

As a working rule, although different animals have and had very different dispersal rates (McKerrow & Cocks, 1976), many faunas appear to be separable into recognisable provinces if the oceanic width is above 1,000 km. If two terranes are at the same latitude (Fig. 2.20b), then the composition of their benthos will be largely the same if the terranes are close to one another. However, if the terranes drift apart, then the larvae of the descendant species of the original benthos will not cross the intervening deeper ocean after a certain period, and thus the discriminating palaeontologist will be able to identify the two terranes as different and separate. Comparably, if two terranes at the same latitude but with different benthos drift towards each other, then the separate provinces recognised by the palaeontologist in the two terranes in the earlier period will gradually merge into a single faunal province in the later period. However, that proximity does not prove that the two terranes actually collided, which needs further evidence, such as 'stitching' granites across the suture zone.

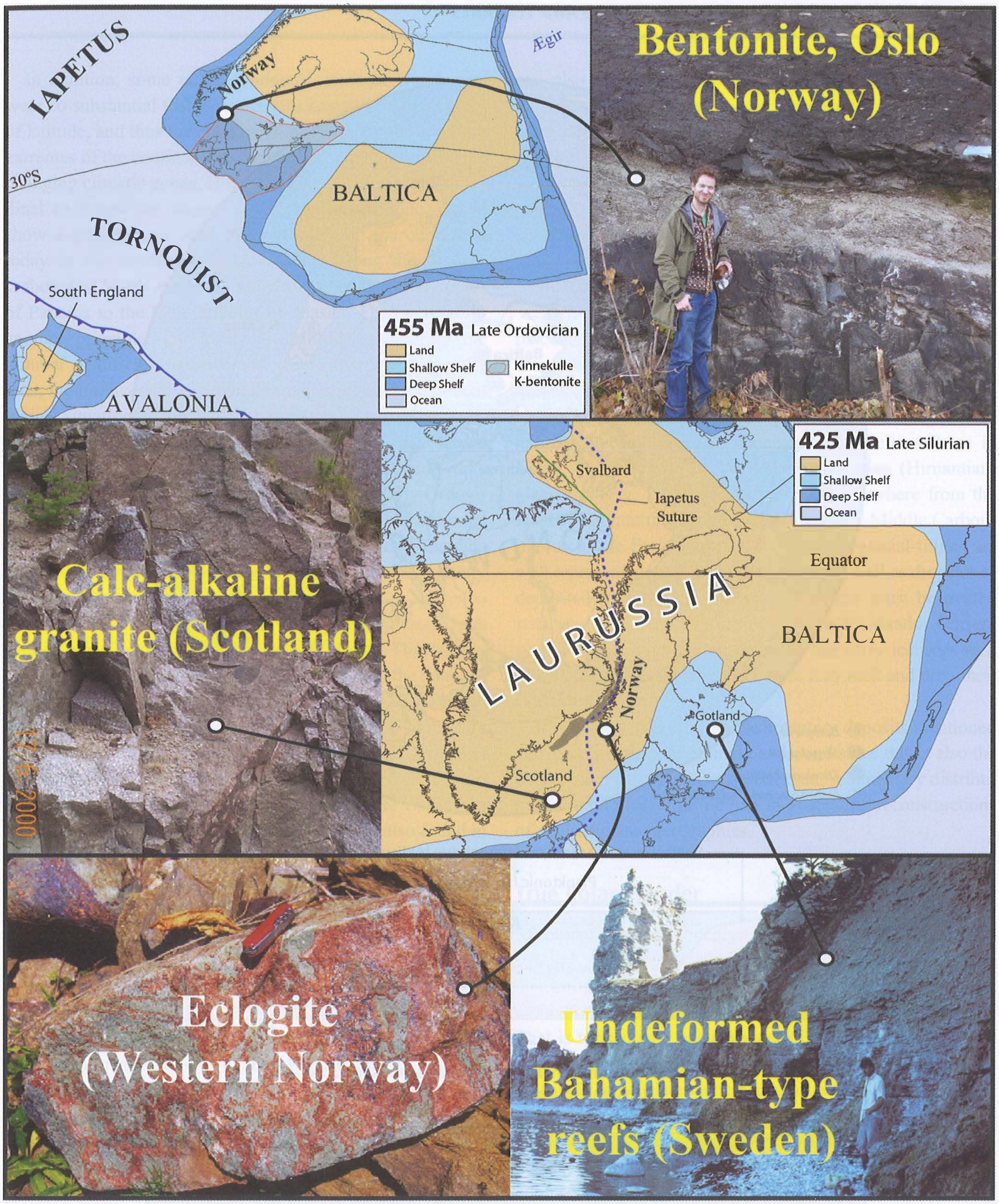

Fig. 2.19 Late Ordovician reconstruction where the Kinnekulle K-bentonite in Baltica is linked to an Avalonian magmatic arc (449–457 Ma), and ash fall-out was transported with westerlies all the way to St Petersburg, Russia. Photo to the left of the Late Ordovician reconstruction shows the bentonite in the Oslo region (grey white layer), dated to around 457 Ma (Tucker & McKerrow, 1995; Svensen et al., 2014). The Late Silurian map (formation of Laurussia after collision of Avalonia and Baltica with Laurentia) is associated with three different pictures, one picture of calc-alkaline granites (425 Ma 'Newer' granite) linked to Iapetus subduction (Avalonian crust) beneath Scotland, a second of high-pressure metamorphic rocks in western Norway linked to subduction of Baltica continental crust beneath Greenland (and subsequent exhumation in the lower Devonian), and a third picture showing undeformed Bahamian-type reefs in the Caledonian foreland. The latter reflect the much better temperatures in southern Scandinavia at this time (subtropical to tropical).

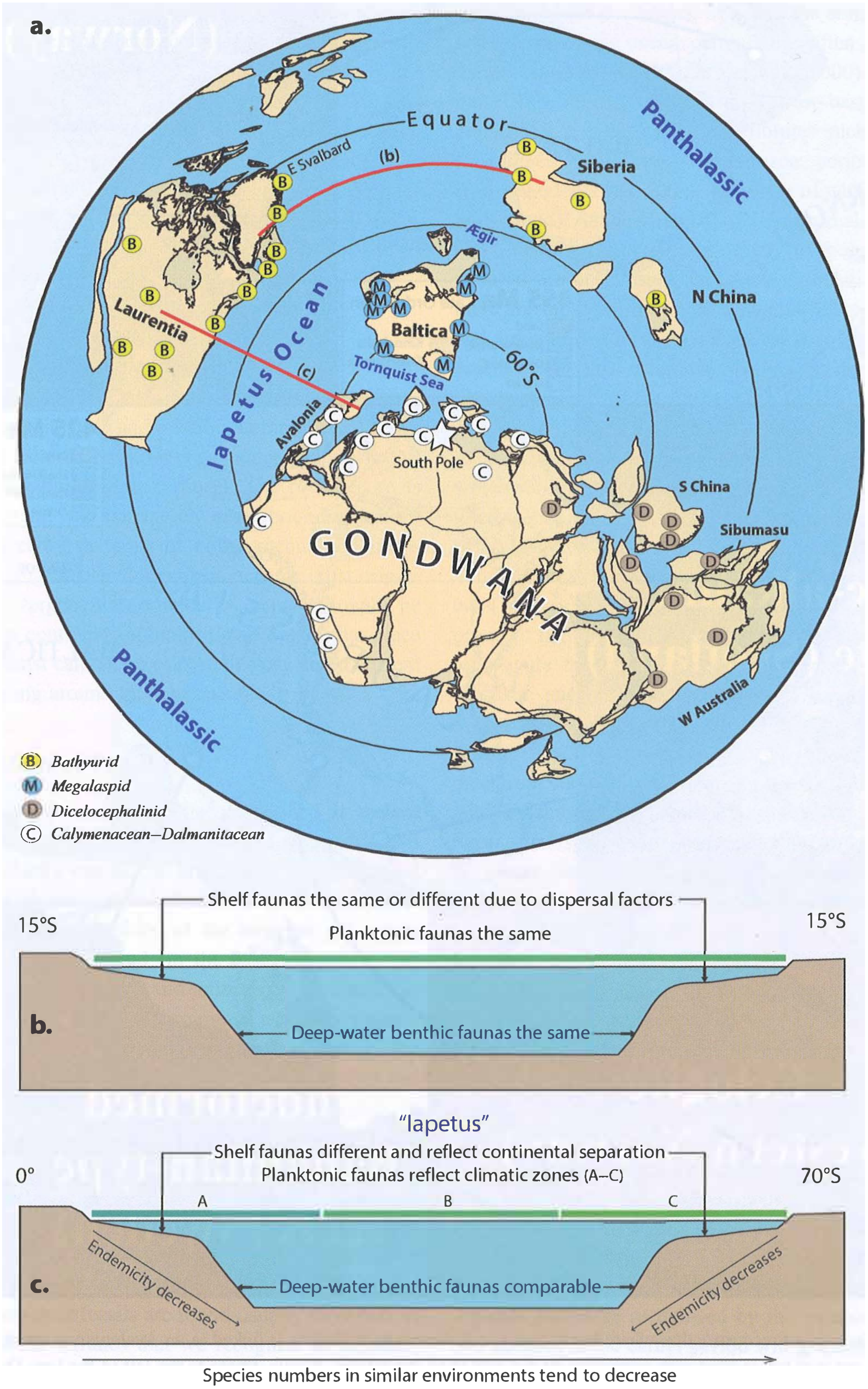

Fig. 2.20 (a) Early Ordovician reconstruction and the distribution of some key trilobite faunas (data from Torsvik et al., 1996 and Cocks & Torsvik, 2002). (b, c) Comparison of faunas found on opposite sides of an ocean at the same latitude or at the same longitude (after Cocks and Fortey, 1982). The red-line east–west profile (about 15° S) and the orthogonal north–south profile (0° to 70° S) in (a) are good analogues. Across the north–south Iapetus Ocean profile, the trilobite shelf faunas differ and reflect continental separation (Bathyurid as opposed to Calymenacean–Dalmanitacean provinces). Conversely, along a profile of constant latitude (arbitrarily shown as 15° S) the trilobite shelf faunas of Laurentia, Siberia, and North China are similar (Bathyurid).

In addition, some palaeocontinents, such as Gondwana, were so substantial that their margins covered many degrees of latitude, and thus the benthos at the northern and southern extremes of the continent can be very different, reflecting the changing climatic zones. However, between these two latitudinal extremes the faunas at intermediate latitude should show a gradation or cline, comparable with the cline seen today in the benthic molluscan faunas along the western seaboard of North America, which stretches from the tropics of Panama to the high latitudes of Alaska. That is allied to another principle: the lower the latitude, the larger the number of different species and genera that will be found; thus, the biodiversity is generally greater (in equivalent ecological situations) the nearer the Equator.

An integrated approach of palaeomagnetic and faunal analysis is applicable for the entire Phanerozoic, but works best for the Early Palaeozoic and, notably, the Early Ordovician (Fig. 2.20a). At that time, Gondwana stretched from the South Pole (Africa) to 20° north of the Equator (Australia and East Antarctica), Baltica occupied intermediate southerly latitudes, separated by the Tornquist Sea, whereas Laurentia straddled the Equator. Laurentia was separated from both Baltica and Gondwana by the Iapetus Ocean. The Iapetus Ocean (~5,000 km across the British sector) and the adjacent Tornquist Ocean (~1,100 km between southern Baltica and south-central Europe) were at their widest. This is probably why benthic trilobites from Laurentia (Bathyurid Province) and north-west Gondwana (Calymenacean Dalmanitacean Province) are so markedly different from those of Baltica (Megalaspid Province). Bathyurid trilobites are also found in Siberia and North China but those continents were located at low latitudes (as was Laurentia), thus explaining the similarity in shelf fauna, although some authors had previously placed Siberia much closer to Laurentia in their reconstructions, partly because of the bathyurid fauna.

Sediment Distributions and Climate Patterns

Other semi-quantitative or qualitative methods, for example the distribution of latitude-sensitive and climate-dependent rock types, have also proved useful in deciphering old geographies, and they, like fossils, can also have the advantage of being derived from data gleaned from rocks that have suffered from much subsequent tectonic activity, in contrast to palaeomagnetism, when the original remanent magmatism has been overprinted and eradicated by later heating.

Carbonate buildups, often termed bioherms or reefs, are widespread throughout Phanerozoic rocks. However, they were largely laid down within tropical to subtropical latitudes (Fig. 2.21), and thus their distribution in ancient times can also be a useful check on the signals derived from palaeontological and other data. Comparably, evaporites are most usually found in belts on either side of the Equator (the subtropics), and so their presence questions the reality of reconstructions that show them at high latitudes. Conversely, coal deposits are commonly confined to the Equator (wet conditions, Fig. 2.21) or the northerly or southerly wet-belts at intermediate to high palaeolatitudes (Scotese & Barrett, 1990; Torsvik & Cocks, 2004; Boucot et al., 2013).

The recognition of glacial deposits has been important in placing continents since Wegener's (1915) original work. Much direct evidence of glaciers, such as eskers and drumlins, is rarely preserved in rocks older than the Pleistocene, but magnificent glacial striated pavements are known from various Precambrian glacial episodes, as well as those in North Africa caused by the latest Ordovician (Hirnantian) glaciation (Fig. 2.21), and in India and elsewhere from the lengthy but intermittent glaciations from the Middle Carboniferous to the Early Permian. In addition, glacial tillites are well represented in rocks of many ages, as well as dropstones deposited by icebergs. However, the latter must be treated with caution since, for example, the cold Labrador Current on the eastern side of Canada today can carry icebergs well down into temperate latitudes before they melt and drop their contained debris.

It is notable that all those sedimentary deposits mentioned above only reflect latitudinal bands, and since this is also the chief output from palaeomagnetic data, sedimentary distribution seldom plays a prime part in generating reconstructions of ancient palaeogeographies.

True Polar Wander

Motion of continents relative to the Earth's spin axis may be not only the motion of individual continents ('continental drift' as we have addressed so far), but also rotation of the entire solid Earth (crust and mantle) relative to its spin axis. That is termed true polar wander (TPW) and has been proposed as an explanation for such disparate phenomena as unusually rapid plate velocities, sea-level variations, climate changes, and geomagnetic reversal frequency.

TPW arises from the gradual redistribution of density heterogeneities within the mantle and corresponding changes in the planetary moment of inertia (Goldreich & Toomre, 1969; Steinberger & Torsvik, 2010). To establish the magnitude of TPW with confidence, the absolute velocity field and the plate geometry for both continental and oceanic lithosphere are required. That is difficult for pre-Cretaceous time and estimates of the relative magnitude of TPW must therefore rely on continental palaeomagnetic data (Fig. 2.23). In

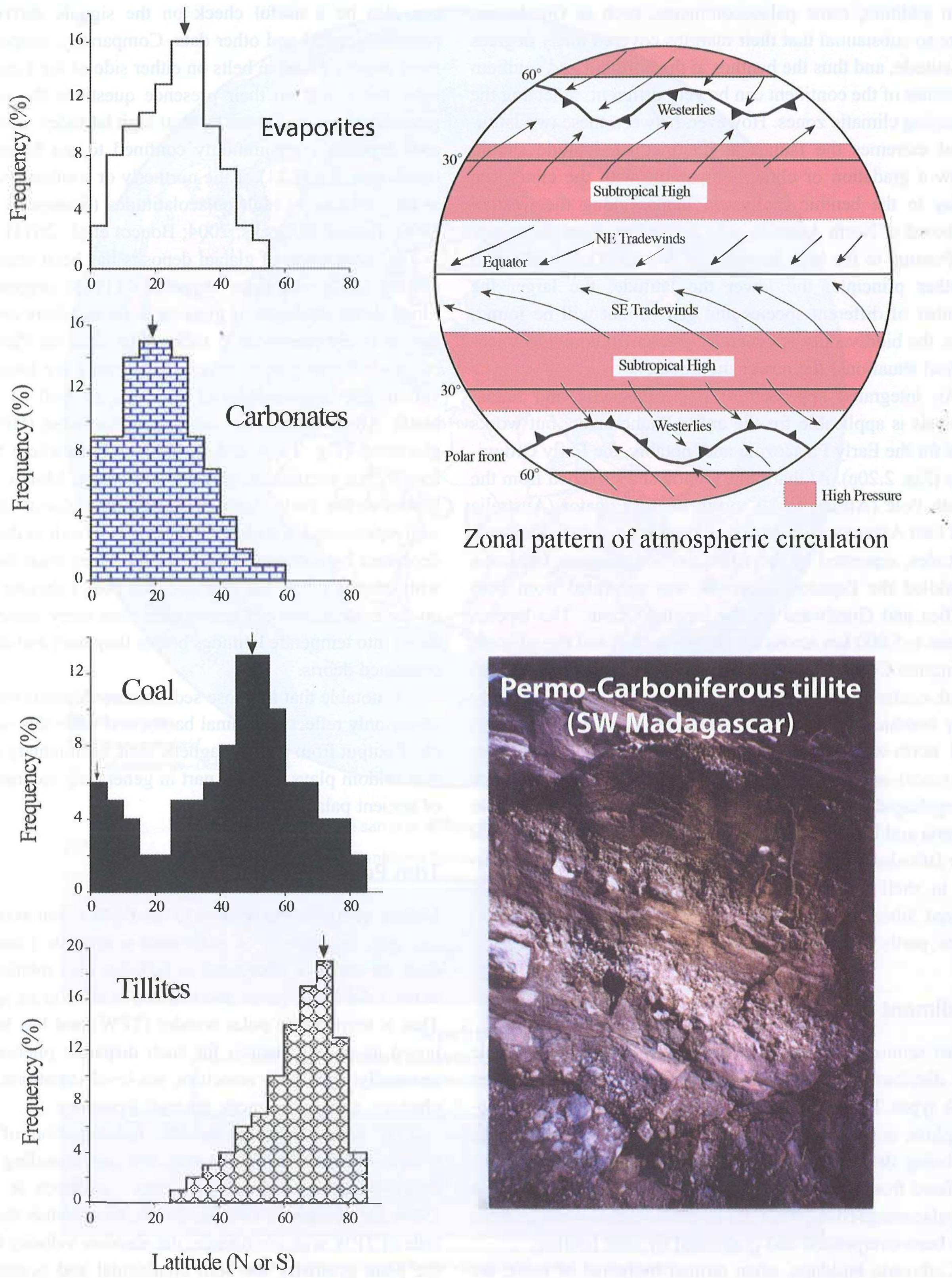

Fig. 2.21 Mesozoic and Cenozoic distributions of evaporites, carbonates, coal, and tillites. The horizontal axis is latitude for both hemispheres. Data in Scotese & Barrett (1990); pattern of zonal atmospheric circulation after Parrish (1982) and Scotese & Barrett (1990).

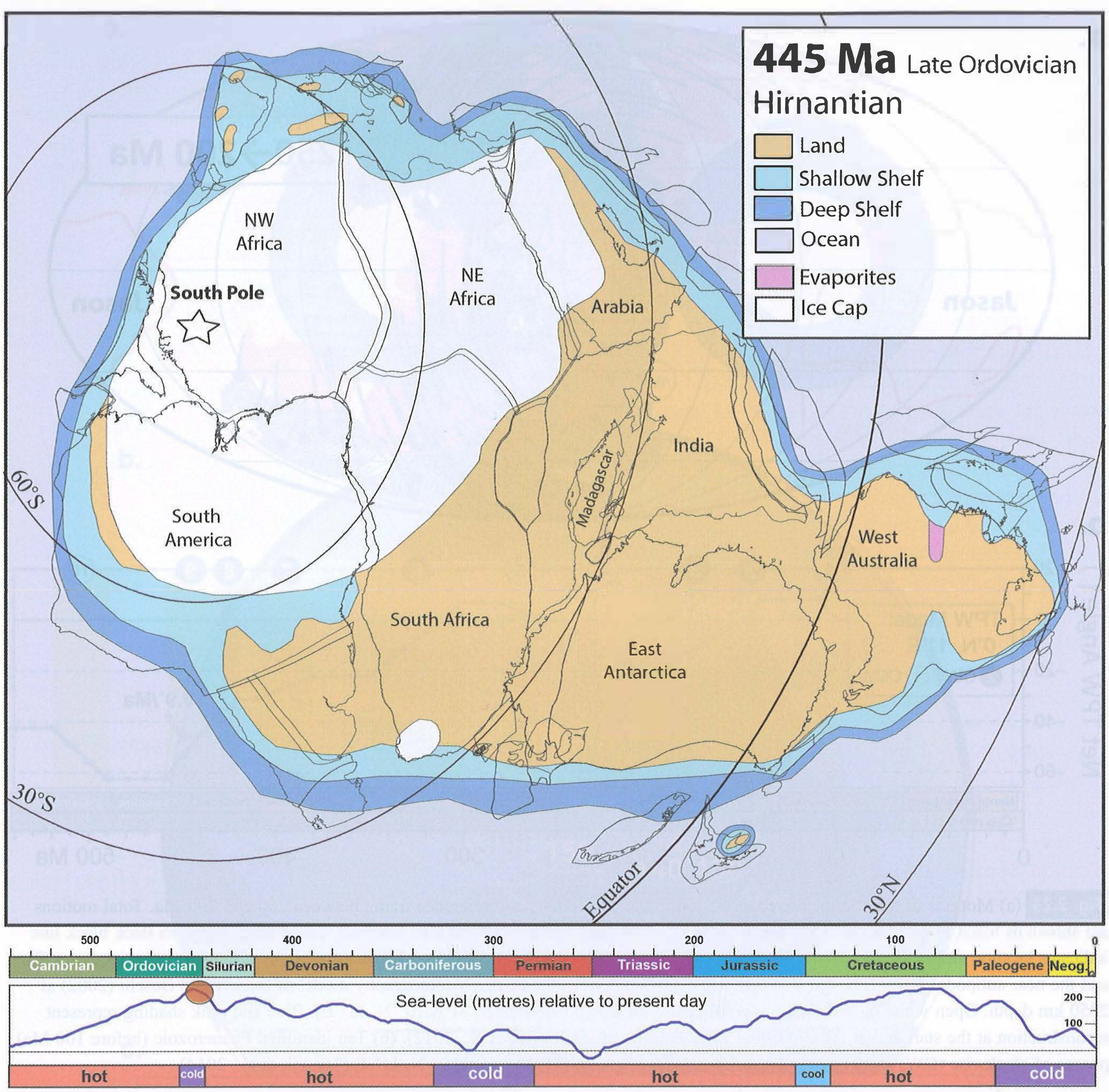

Fig. 2.22 Gondwana in the Latest Ordovician (Hirnantian: 445 Ma), showing the extent of the glacial ice cap. Bottom: Phanerozoic time scale (Endpaper), sea-level variations (Haq & Al-Qahtani, 2005; Haq & Shutter, 2008), and icehouse (cold) and greenhouse (hot) conditions.

spite of those difficulties, one can attempt to determine the magnitude of TPW by extracting the coherent (mean) rotation of all the continents around their common centre of mass in the palaeomagnetic reference frame of Steinberger and Torsvik (2008) (Fig. 2.23). Using that method, ten phases of slow and oscillatory TPW (around ~11° E and 191° E at the Equator) have been modelled for the entire Phanerozoic. Adding dense material in the upper mantle must be a prime candidate for causing TPW, and we expect that intermediate- to high-latitude subduction would preferentially induce TPW so that subduction zones shift towards the Equator, possibly with some time delay (Torsvik et al., 2014).

Attempts to link Earth's ancient LIPs and kimberlites (using palaeomagnetic data) to its interior require that TPW is accounted for. Because TPW is defined as the *rotation of the crust and mantle* (around a point at the Equator), TPW

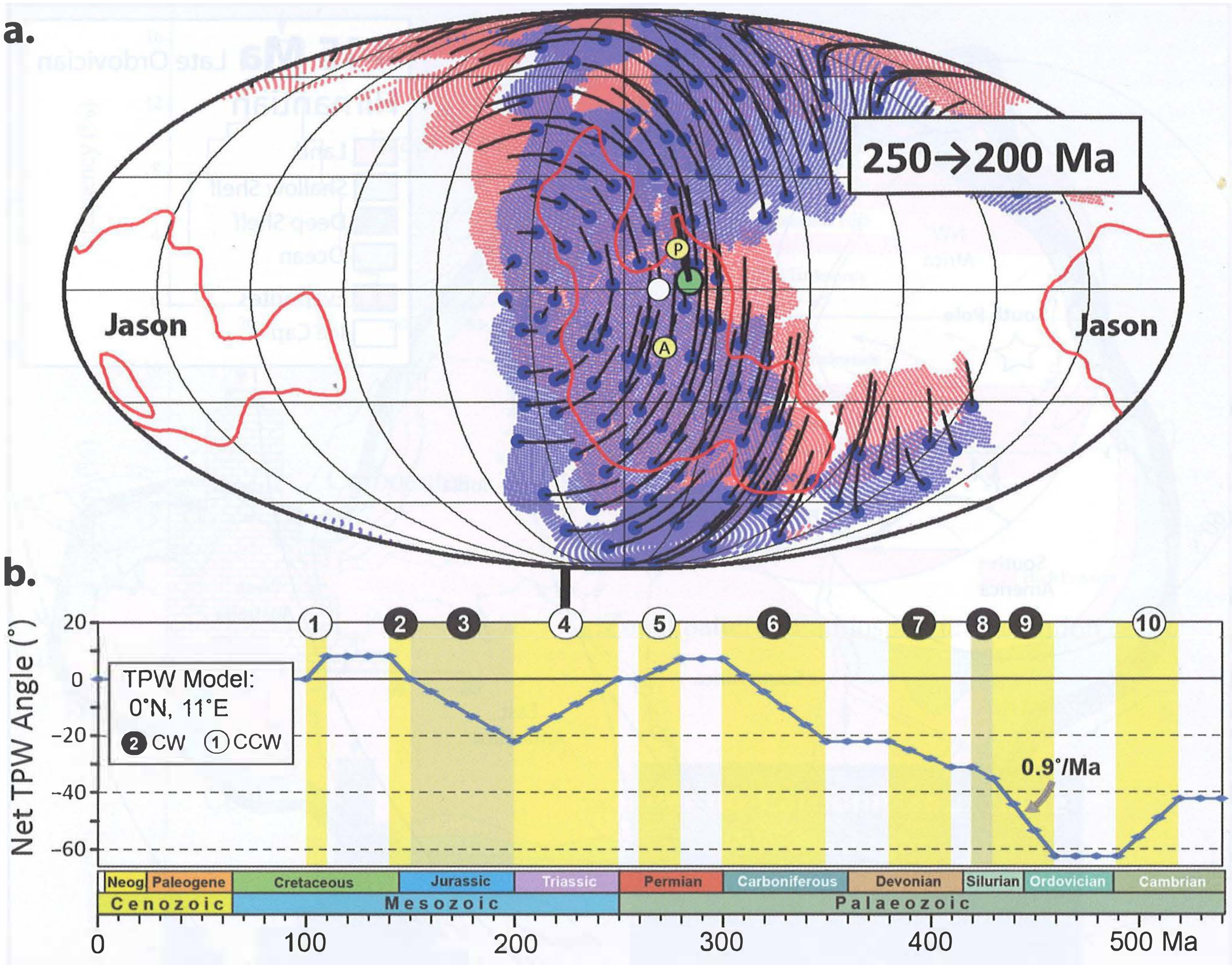

Fig. 2.23 (a) Motions of the continents reconstructed in the palaeomagnetic reference frame between 250 and 200 Ma. Total motions are shown as black lines, connected to blue dots (locations at the beginning of the time interval). Large green dot with thick black line indicates location and motion of the centre of mass of 'all' continents. Yellow dots (A and P) are the centre of mass or its antipode for Tuzo and the near antipodal Jason. The red line is the 1% slow contour in the SMEAN tomography model of Becker and Boschi (2002) at 2850 km depth. Open white circle is the preferred centre for true polar wander, TPW (0° N, 11° E). Blue and pink shading represent reconstruction at the start and at the end of the TPW episode (after Torsvik et al., 2012). (b) Ten identified Phanerozoic (before 100 Ma) phases of clockwise (CW) and counter-clockwise (CCW) rotations (TPW) around 0° N, 11° E (Torsvik et al., 2014).

correction may appear out of order since during a TPW event both the continent (with its embedded LIPs and kimberlites) and Tuzo and Jason must have rotated in the same manner (Fig. 2.24a). However, in such correlative exercises we compare surface reconstructions with fixed (present-day) features in the mantle (e.g. tomography) and thus the palaeomagnetic reconstruction *must* be corrected for TPW. Fortunately, the net cumulative effect of TPW through time (at least since the Late Palaeozoic) is at certain periods zero (e.g. Late Permian and Late Jurassic), or very small (Fig. 2.23b). Thus TPW-corrected or not corrected reconstructions can be quite similar, but that is not the case for the Early Palaeozoic.

In Fig. 2.23 TPW was estimated purely based on palaeomagnetic data; the axis of TPW rotation varies at certain intervals but averages to about 11° E (and 191° E) at the Equator (Fig. 2.24b) between 320 and 100 Ma, which was used as a constant value (Torsvik et al., 2012). TPW can also be calculated as the difference between a global moving hotspot reference frame and the palaeomagnetic one. Between 120 and 100 Ma calculated TPW is almost the same as that calculated from palaeomagnetic data alone, and, for the past 40 million years, the axis of TPW rotation is also close to that estimated from palaeomagnetic data. There is, however, a major deviation between 90 and 40 Ma (Late

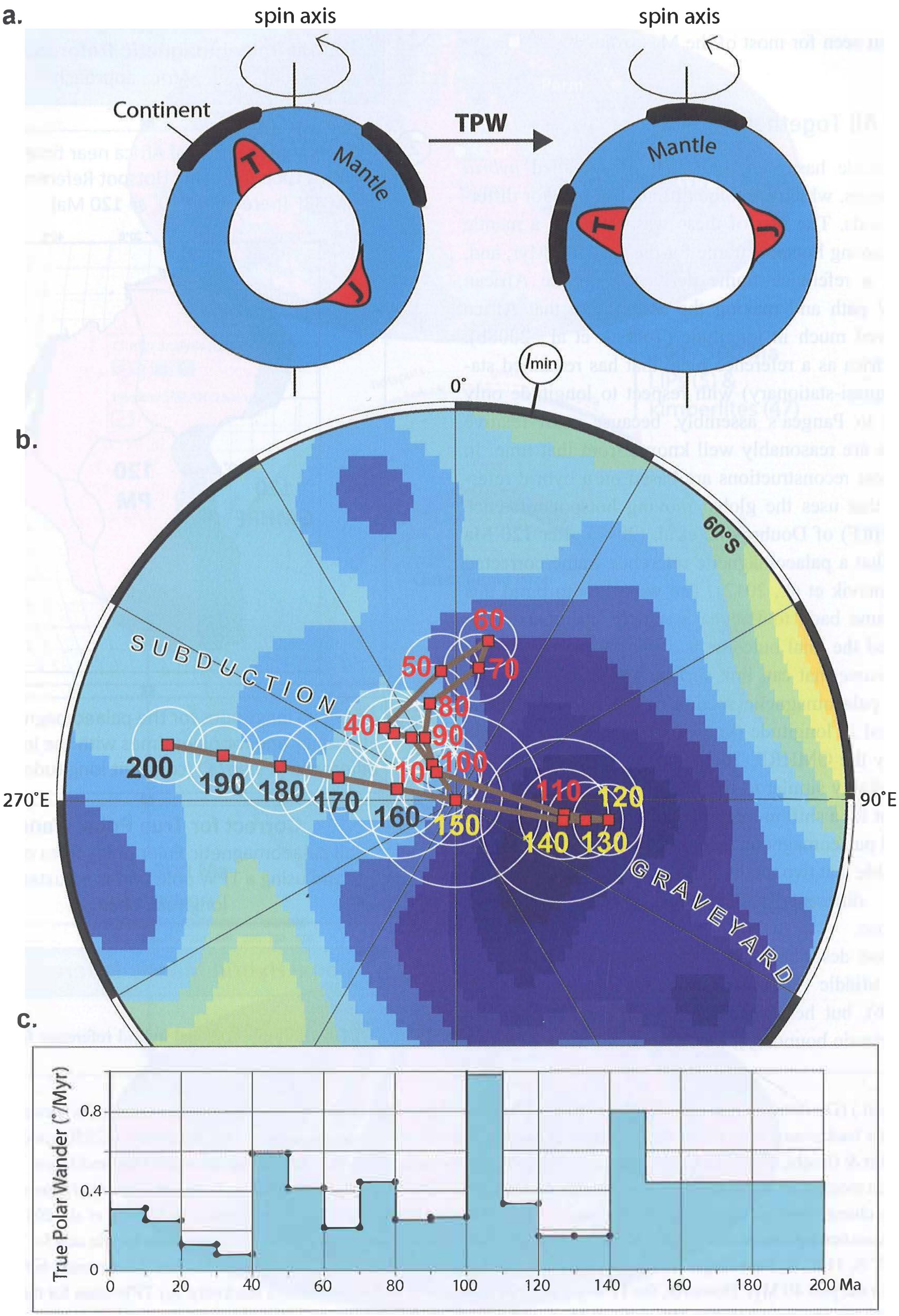

Fig. 2.24 (a) During a true polar wander (TPW) event both continents and the LLSVPs (Tuzo and Jason) will rotate the same amount (lower panel) around a rotation pole at the Equator. (b) TPW paths estimated from coherent rotation of all continents around an equatorial axis from only palaeomagnetic data (200–130 Ma) and from palaeomagnetic data (Torsvik et al., 2012) rotated into a GMHRF

Cretaceous to Middle Eocene), where TPW is almost orthogonal to that seen for most of the Mesozoic.

Putting It All Together

The past decade has seen the dawn of so-called *hybrid reference* frames, which combine different frames for different time periods. The first of these was based on a mantle reference (moving hotspot) frame for the past 100 Myr, and, before that, a reference frame derived from the African global APW path and making the assumption that Africa has not moved much in longitude (Torsvik et al., 2008b). Choosing Africa as a reference plate that has remained stationary (or quasi-stationary) with respect to longitude only works back to Pangea's assembly, because most relative plate circuits are reasonably well known from that time. In this book most reconstructions are based on a hybrid reference frame that uses the global moving hotspot reference frame (GMHRF) of Doubrovine et al. (2012) after 120 Ma and before that a palaeomagnetic reference frame corrected for TPW (Torsvik et al., 2012). The workflow to build this reference frame back to Pangea assembly is illustrated in Fig. 2.25, and the final outcome is a *Global Hybrid Mantle Reference Frame* that can link surface and deep Earth processes. The palaeomagnetic section of the reference frame was calibrated in longitude (known movement in longitude of Africa) by the GMHRF. The palaeomagnetic reconstruction is remarkably similar to the GMHRF reconstruction for Africa except for a shift in longitude of about 10° that is used to correct all palaeomagnetic reconstructions before 120 Ma. It is remarkable that two totally independent reference frames (and very different assumptions) produced similar reconstructions.

The method described above can potentially be carried back to the Middle Carboniferous at 320 Ma (e.g. Torsvik et al., 2008b), but here we only do this back to 250 Ma (Permian–Triassic boundary); before then we use a different

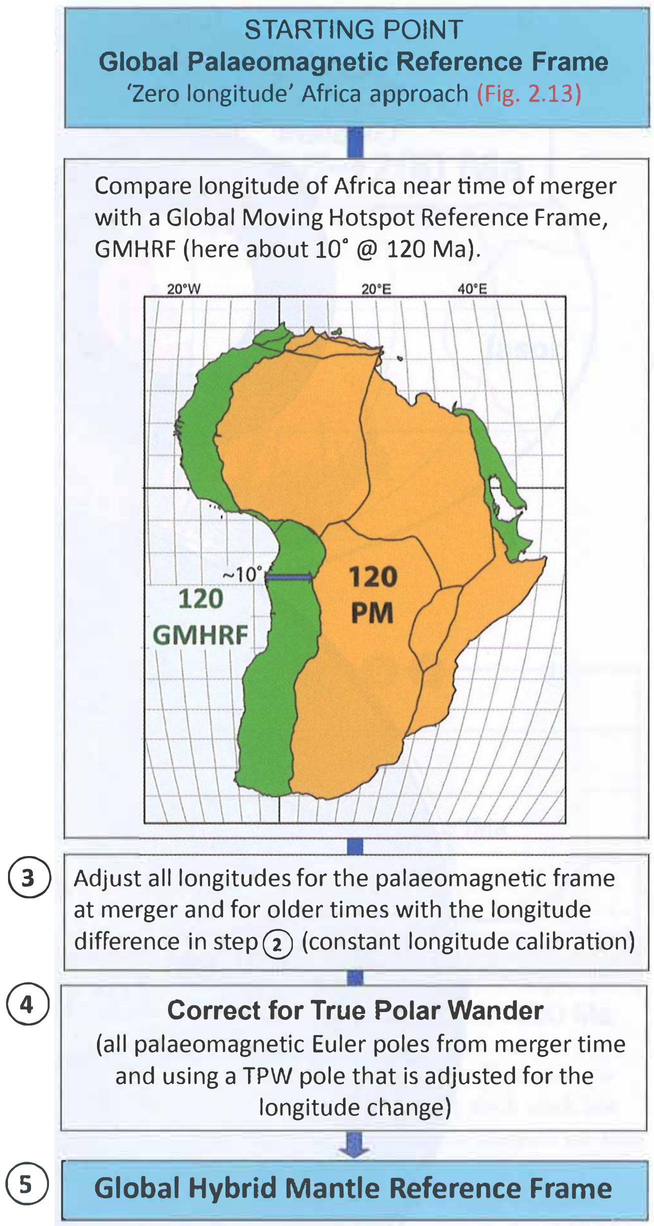

Fig. 2.25 How to build a global hybrid reference frame.

Fig. 2.24 (*cont.*) (Doubrovine et al., 2012) after 120 Ma. The two independent methods yield almost identical results between 120 and 100 Ma. Colour background map shows the variations of S-wave velocity (δV_s) near the core mantle boundary at 2850 km depth (SMEAN model of Becker & Boschi, 2002). The TPW path is always confined above the high-velocity regions between Tuzo and Jason. The orientation of the minimum moment of inertia axis (I_{min}) of the Earth and therefore TPW is largely controlled by Tuzo and Jason (not shown in this figure), but is likely to change through time due to mass changes from subducted slabs and rising plume heads. In Torsvik et al. (2012) I_{min} was modelled at a constant equatorial location of 11° E (and 191° E) which closely matches the minimum moment of inertia axis for Tuzo and Jason combined (2.7° S, 11.9° E; Steinberger & Torsvik, 2010). I_{min} calculated from the GMHRF closely matches this estimate between 120 and 100 Ma and for the past 40 Myr. However, the TPW path (loop) between 90 and 40 Ma differs markedly. (c) TPW rates for the past 200 Myr. The fastest rates are observed between 100 and 110 Ma (~1°/Myr). A comparable peak is also observed from palaeomagnetic data alone (0.9°/Myr, Torsvik et al., 2012, 2014), and here by comparing a GMHRF and the palaeomagnetic data. The mystical 50 Myr TPW path between 90 and 40 Ma in (b) is not associated with notably higher-than-normal TPW rates (maximum 0.6°/Myr between 50 and 40 Ma). Note that there is only one total average for the whole 200–150 Ma interval, but the actual rates vary. Therefore reconstructions, for example in 10 Myr time intervals and corrected with a constant TPW rate, may result in artificial back-and-forth rotations of all the continents.

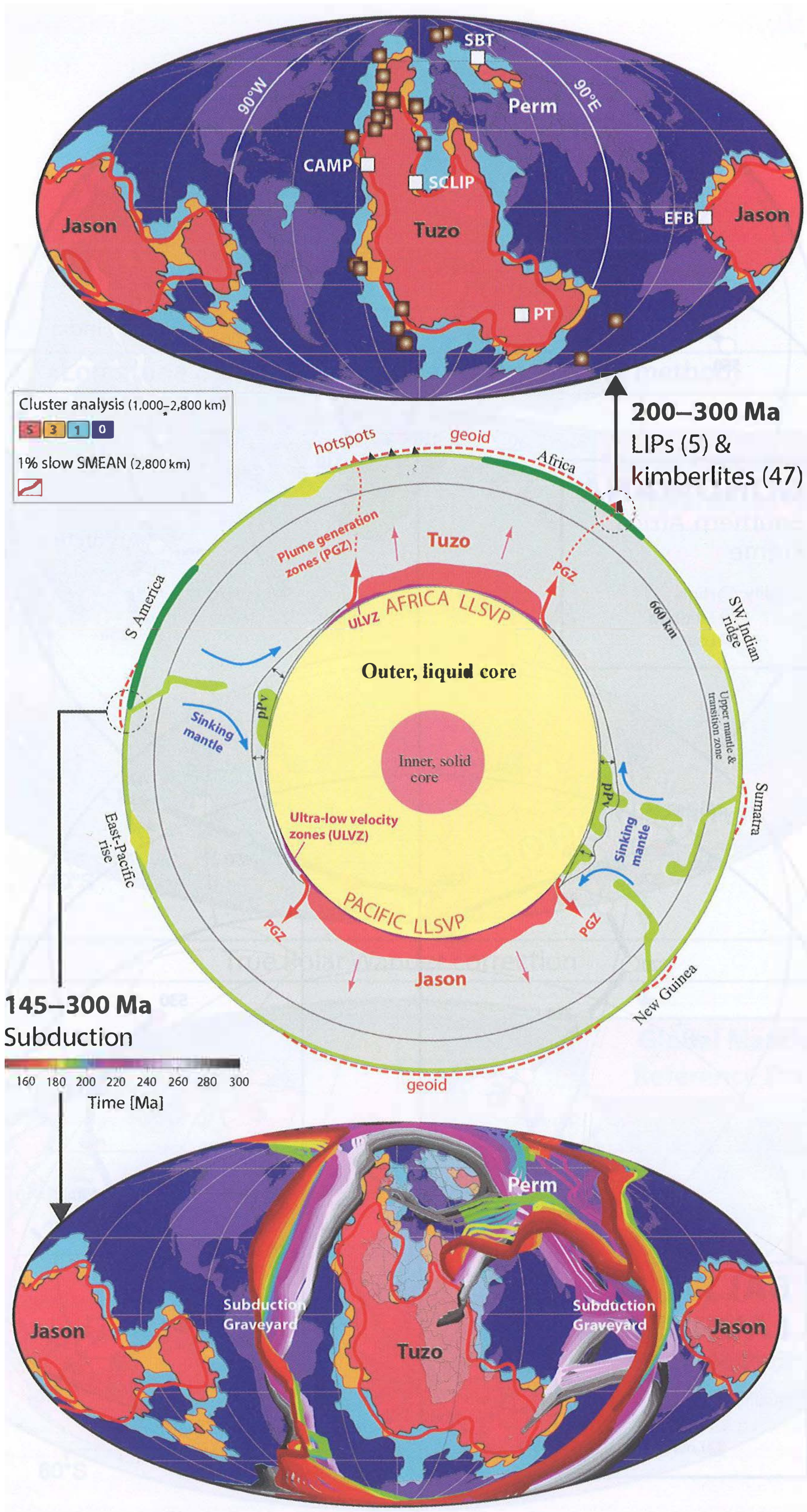

Fig. 2.26 Earth since Pangea: a planet where the geoid is dominated by a degree-2 mode, with elevated regions above large low shear-wave velocity provinces on the core–mantle boundary beneath Africa (Tuzo) and the Pacific (Jason). The edges of these deep mantle bodies (when projected radially to the Earth's surface) correlate with the reconstructed positions of large igneous provinces and kimberlites (top diagram showing LIPs and kimberlites erupted between 200 and 300 Ma) since Pangea formed at about 320 Ma. The geoid is largely a result of buoyant upwellings overlying Tuzo and Jason (thin red arrows), and subduction is largely confined between them (the subduction graveyards, lower diagram with subduction history between 145 and 300 Ma). EFB, Emeishan Flood Basalts; SBT, Siberian Traps; pPv, post-perovskite (bridgemanite).

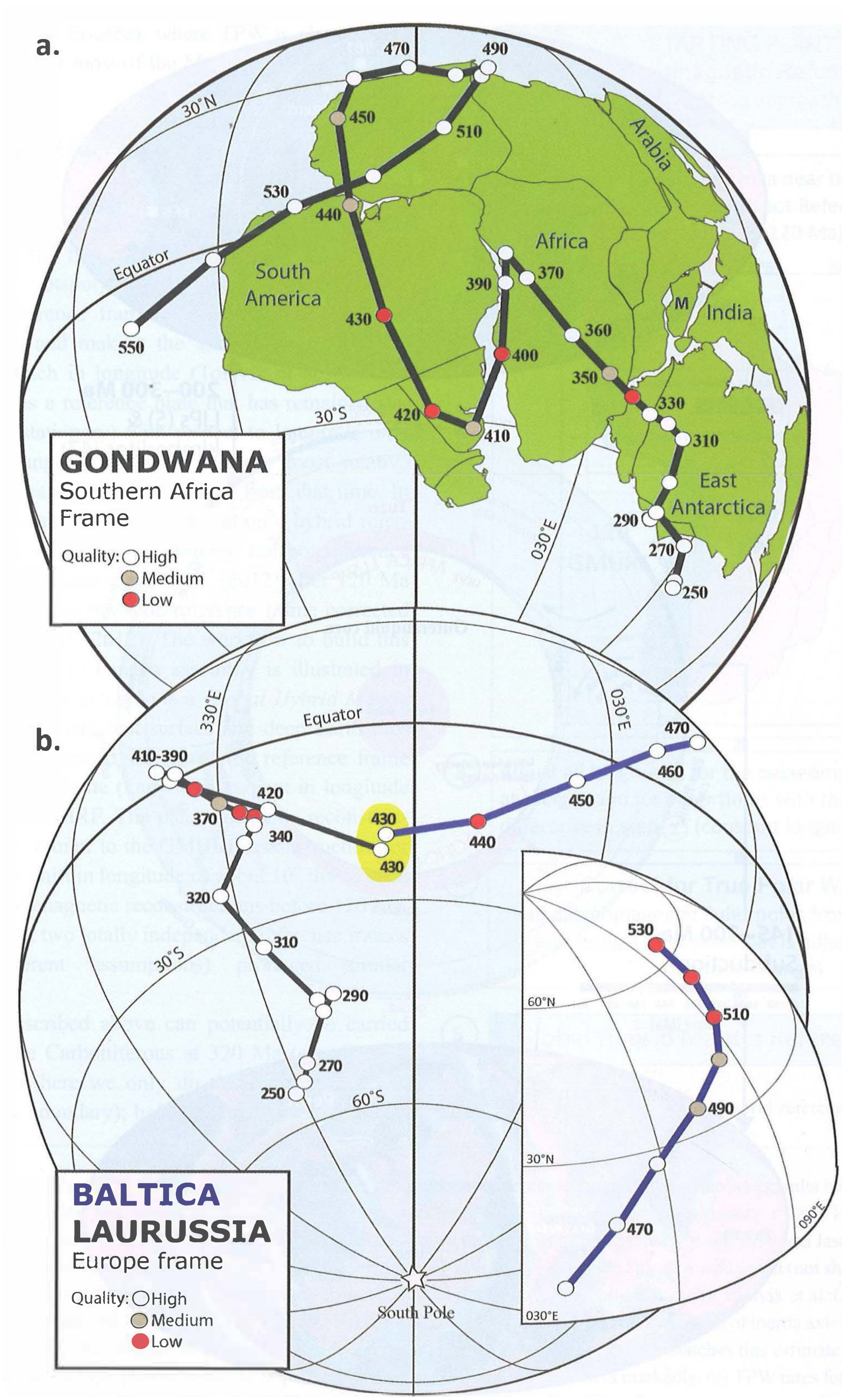

Fig. 2.27 (a) Phanerozoic smoothed spherical fitted apparent polar wander paths for Gondwana (550–250 Ma), Baltica (530–430 Ma), and Laurussia (Baltica/Stable Europe/Laurentia) from 430 Ma after correcting for the opening of the Labrador Sea (65–30 Ma) and the north-east Atlantic (55 Ma to present). Quality/reliability of the mean poles is classified as high, medium (only one pole) or low (purely interpolated).

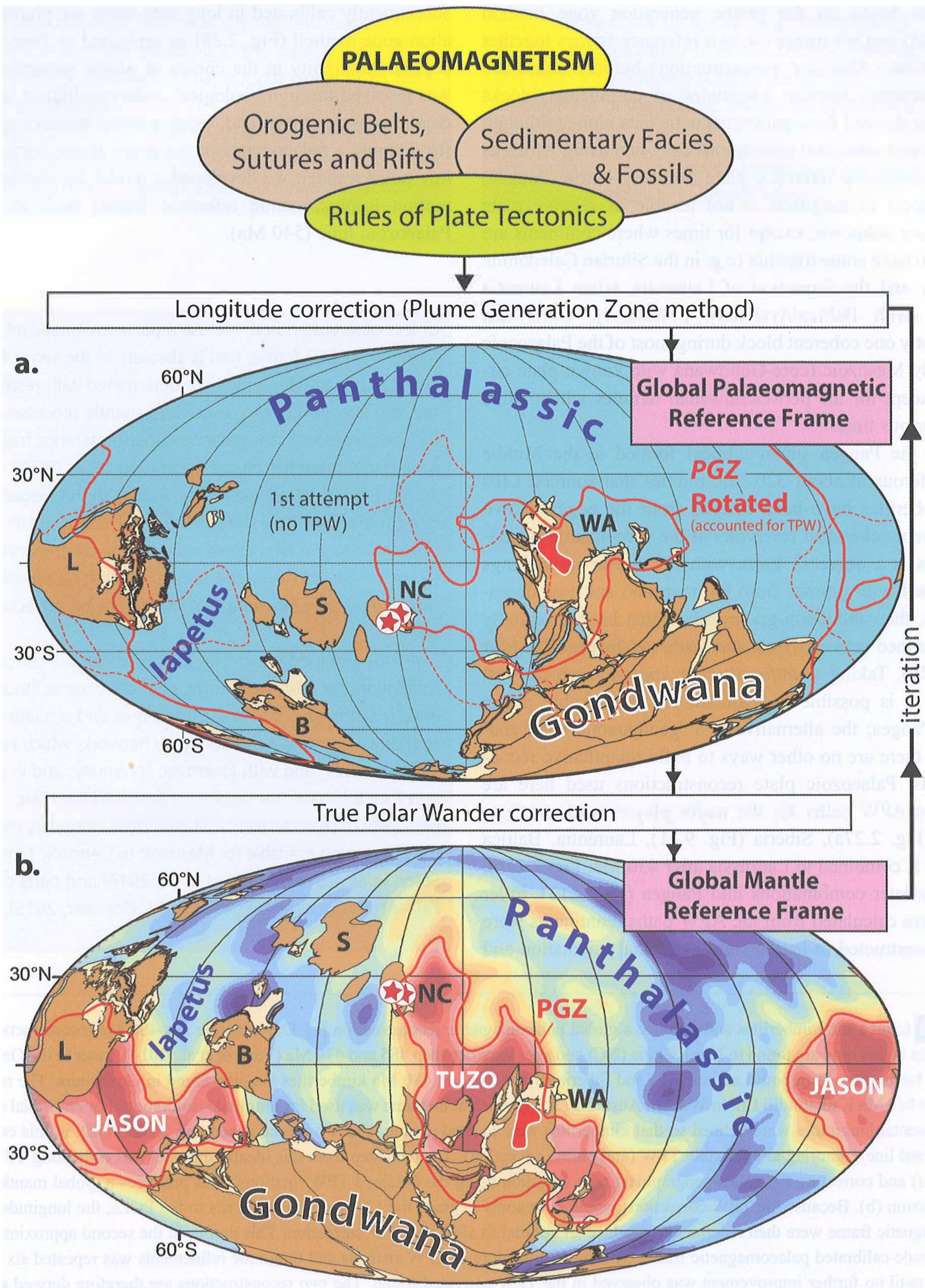

Fig. 2.28 Based on what we know about our planet for the past 320 Myr, notably the surface-to-core mantle boundary correlation (Fig. 2.26), and our knowledge about how true polar wander (TPW) works, we use palaeomagnetic data (constraining latitude and rotation) in concert with geological information to first produce realistic global maps for times before Pangea. We then calibrate longitude with LIPs

technique based on the plume generation zone method (Fig. 2.28) and we merge the two reference frames together at this time. 'Absolute' reconstructions before Pangea are more uncertain because longitudes of continental blocks cannot be derived from palaeomagnetic data alone (although latitudes and azimuthal orientations can), and using Africa as a quasi-stationary reference plate (unlikely before Pangea) with respect to longitude is not tenable as relative plate circuits are unknown; except for times where continents are known to have come together (e.g. in the Silurian Caledonide Orogeny and the formation of Laurussia, when Laurentia collided with Baltica/Avalonia). Fortunately, Gondwana was mostly one coherent block during most of the Palaeozoic and Early Mesozoic (core-Gondwana with known plate circuits) except for the peri-Gondwanan terranes which rifted off at various times.

Since the Pangea supercontinent formed in the Middle Carboniferous at about 320 Ma, plumes that sourced LIPs and kimberlites have been derived from the edges of two stable thermochemical reservoirs at the core–mantle boundary. This is a degree-2 Earth with two major up-wellings (associated with plumes from the margins) and two down-wellings, the subduction graveyards which have essentially been confined between Tuzo and Jason for the past 320 Myr (Fig. 2.26). Taking a *uniformitarian approach* we can test whether it is possible to maintain this remarkable planet before Pangea; the alternative is a 'geodynamic dead end' because there are no other ways to build quantitative reconstructions. Palaeozoic plate reconstructions used here are based on APW paths for the major players such as Gondwana (Fig. 2.27a), Siberia (Fig. 9.11), Laurentia, Baltica (Fig. 2.11; combined to Laurussia after 430 Ma; Fig. 2.27b), and their later combinations into Pangea (Fig. 2.13). Euler poles were calculated from the APW paths; continents were then reconstructed in latitude and azimuthal orientation and subsequently calibrated in longitude using the plume generation zone method (Fig. 2.28) as explained in Torsvik et al. (2014). Ambiguity in the choice of plume generation zone was resolved through geological, palaeontological, and kinematic considerations; and, using a novel iterative approach for defining a palaeomagnetic reference frame corrected for true polar wander, we developed a model for absolute plate motion (global mantle reference frame) back to earliest Palaeozoic time (540 Ma).

Unless otherwise noted, we use a palaeomagnetic reference frame, the CEED frame, that is absolute in the sense that both latitude and longitude are determined with respect to the spin axis. In order to relate deep mantle processes to surface processes in the palaeomagnetic reference frame, we have also rotated the plume generation zones (PGZs) to account for TPW (red lines in Fig. 2.28a). In this elegant way, one can perceive how the surface distributions of LIPs (Appendix 1) and kimberlites relate to the deep mantle (Torsvik et al., 2014), at the same time plotting climatically sensitive sedimentary data that should not be corrected for TPW.

A full-plate model (e.g. Fig. 2.18a), unlike the continental rotation model described above, contains oceanic lithosphere (mostly synthetic before the Cretaceous) and requires an explicitly prescribed plate boundary network, which evolves independently, and with kinematic continuity, and in such a way that the collective system conforms to the basic principles of plate tectonics. Such a plate boundary model is now becoming available for Mesozoic to Cenozoic times (e.g. Seton et al., 2012; Shephard et al., 2014) and parts of the Palaeozoic (Domeier & Torsvik, 2014; Domeier, 2015), and is

Fig. 2.28 (*cont.*) and kimberlites and produce a global palaeomagnetic reconstruction (a). Our example is a 480 Ma reconstruction and kimberlites at this time are found in North China (NC) and ages vary between 485 and 474 Ma (Torsvik et al., 2014). Later in the Ordovician there are kimberlites from both Laurentia (L) and Siberia (S), and before 480 Ma kimberlites are also found in Gondwana. The map also shows the 511 Ma Kalkarindjii LIP in Western Australia (WA), which at that time was used for longitude calibration. For our initial model in (a), continental longitudes were defined so that kimberlites were located directly above a plume generation zone (PGZ), in this case Tuzo (stippled red line), ignoring any possible TPW (and plume advection). The next step from this idealised model was estimating TPW (as in Fig. 2.23a) and correcting the palaeogeographical reconstruction using the obtained TPW rotations. This produces a global mantle reconstruction (b). Because the TPW corrections would commonly degrade the LIP and kimberlite fits to the PGZs, the longitudes in the palaeomagnetic frame were then redefined to produce an optimal fit after the TPW correction. This produced the second approximation for the longitude-calibrated palaeomagnetic frame. The entire procedure of TPW analysis and longitude refinements was repeated six times in this case until no further improvement was observed in the TPW-corrected frame. The two reconstructions are therefore derived after the iteration procedure and the kimberlite fits are for both reconstructions. Note that in (a) the PGZ has been rotated according to the amount of TPW. In our global Palaeozoic model used in the book we did this procedure in 5 Myr steps from 540 to 250 Ma (Torsvik et al., 2014). B, Baltica.

used in this book whenever available. As stated above, practically all our reconstructions in this book use a palaeomagnetic reference frame, but our global maps from Triassic onwards (Figs. 11.1, 12.1, 12.3, 13.1, 13.2, 14.1, 15.1, and 15.2) are generated with GPlates using data supplied in Shephard et al. (2014). The reference frame there (termed EARTHBYTE mantle frame) *resembles* the global hybrid mantle frame of Torsvik et al. (2008b), some plate fits may also differ from the author's preference, and these figures mainly serve to portray the development of the oceanic lithosphere (Müller et al., 2008) in a vivid way.

GPlates rotation files and added information are available at http://www.earthdynamics.org/earthhistory/.